

Department of Bioproducts and Biosystems

Xueyao Ge

Regenerated cellulose films from a binary solvent system

Submitted for inspection on 30, June, 2018

Espoo, Finland

Supervisor (Chalmers) Professor Christian Müller

Supervisor (Aalto) Professor Herbert Sixta

Instructor (Aalto) Simone Haslinger

Abstract

Aalto University

School of chemical technology – Department of bioproducts and biosystems

Master's Program in Nordic Five Tech- Polymer Engineering

Author: Xueyao Ge

Title: *Regenerated cellulose films from a binary solvent system*

Number of pages: 56

Date: 30.06.2018

Language: English

Supervisors: Prof. Christian Müller Prof. Herbert Sixta

Advisors: Ph.D Simone Haslinger

Abstract

In this thesis, the cellulose films regenerated from various solvent systems and the main properties of such films were reviewed based on the recent literatures. Among the different solvent systems, it has been found that a certain class of ionic liquids are more environmentally friendly, since the processing conditions of cellulose are much milder and only small amounts of degradation products are generated from the solvent and solute. In general, the regenerated cellulose films from ionic liquids are transparent with relatively high mechanical properties. In addition to their biodegradability and thermal stability, the regenerated cellulose films are considered to have a great potential to be used as packaging materials. This thesis focused on the dissolution of birch prehydrolyzed kraft pulp (Enocell) in 1,5-diazabicyclo [4.3.0] non-5-ene acetate ([DBNH]OAc) and the fabrication of regenerated films by casting without extensive stretch. Various cellulose concentrations, different coagulation media and different drying methods were explored to optimize the process, and to improve the comprehensive properties of the regenerated films. It was found that the best films were obtained from a concentration of 5.6 wt% to 5.8 wt%. The most appropriate regeneration conditions were coagulation in aqueous ethanol (80%) and drying at a constant humidity of 30% RH (relative humidity) and at a temperature of 23 °C. With slight stretching, these films showed a high tensile strength of 75 MPa, an elongation of 3% and a Young's Modulus of 6.5 GPa. The optical transmittance was over 88%, which was comparable to that of the commercial cellophane. 10 wt% Betulin based on Enocell pulp was mixed with the solution, resulting in an enhanced contact angle from 27.5° to 71.5°, due to the aggregates of Betulin dispersed evenly on the surface. However, both films (with and without the addition of Betulin) showed poor water vapor barrier properties, which were between 3000 and 4000 $g \cdot \mu m / m^2 \cdot day \cdot kPa$.

Keywords: Ionic liquid, [DBNH][OAc], regenerated cellulose films, mechanical properties, optical transmittance, coagulation, drying methods

Acknowledgements

I would like to extend my gratitude to the many people who assisted to bring this research project completed. First, I thank Professor Herbert Sixta, for the opportunity to accomplish my research in the research group, and the opportunity to visit Institute of Biopolymer and Fibers in Poland. I am so deeply grateful for his help, professionalism, valuable guidance and financial support throughout this project and through my entire program of study and research that I do not have enough words to express my deep and sincere appreciation. In addition, I would like to thank Professor Christian Müller in Chalmers University of Technology to provide his professional advices and support on thesis writing.

I would like to thank PhD candidate Simone Haslinger for encouraging, inspiring and instructing me. She also gave me advices about my thesis writing. I am grateful that I had other PhD candidates in the research group, Most Moriam, Oona Korhonen, Hilda Zahra and Leena Katajainen, as well as Dr. Michael Hummel support along this journey. It would not have been possible without their support and guidance. I would like to thank you for always having an answer to the unending stream of questions and pushing me to the right track. I must thank Dr. Dariusz Wawro in Institute of Biopolymer and Fibers in Poland for his consulting and sharing his experience during the time that I was working on my thesis.

At the end I must send my regards to Ms. Rita Hatakka who provided assistance to run my lab tests and analyses.

Table of Content

1.	Introduction.....	7
1.1	Research objectives and questions.....	7
1.2	Structure of the thesis.....	8
2.	Literature review.....	9
2.1	Cellulose solvents.....	11
2.2	Ionic liquids.....	12
2.2.1	[DBNH][OAc].....	13
2.3	Regenerated cellulose materials.....	14
2.3.1	Regenerated cellulose films and membranes.....	15
2.3.2	Regenerated cellulose fibers.....	19
2.3.3	Other regenerated cellulose materials.....	19
2.4	Modification of regenerated cellulose films.....	19
3.	Materials and methods.....	20
3.1	Materials.....	20
3.2	Methods.....	20
3.2.1	Dissolution of cellulose.....	21
3.2.2	Preparation of regenerated cellulose films.....	21
3.3	Characterizations.....	25
4	Results and discussion.....	28
4.1	Influence of concentration and coagulated bath on film properties.....	29
4.2	The rheological properties of cellulose/[DBNH]OAc solutions.....	29
4.2.1	Steady shear viscosity.....	30
4.2.2	Storage modulus and loss modulus.....	30

4.3	Characterization of regenerated cellulose films	31
4.3.1	MMD and Degree of polymerization	31
4.3.2	Surface morphology and transparency	33
4.3.3	Mechanical properties.....	38
4.3.4	Thermal stability.....	40
4.3.5	Water vapor permeability	41
4.3.6	Hydrophilicity.....	42
4.3.7	Efficiency of remove IL ([DBNH]OAc) by deionized water	44
5.	Conclusion	44
	Reference	47
	Appendix 1. Mechanical properties of regenerated films from recent publications.	47
	Appendix 2. Regenerated cellulose films produced by spinning in detail	60

List of abbreviations

DP	Degree of polymerization
NMMO	N-methylmorpholine-N-oxide
[bmim]Cl	1-butyl-3-methylimidazolium chloride
[amim]Cl	1-allyl-3-methylimidazolium chloride
[DBNH][OAc]	1,5-diazabicyclo[4.3.0]non-5-ene acetate
PP	Polypropylene
RCF	Regenerated cellulose films
DMAc/LiCl	N,N-dimethylacetamide/ lithium chloride
(DMI)/LiCl	1,3-dimethyl-2-imidazolidinone/ lithium chloride
GPC	Gel permeation chromatography
MMD	Molar mass distribution
WVTR	Water vapor transmission rate
WVP	Water vapor permeability
RH	Relative humidity

1. Introduction

1.1 Research objectives and questions

Green chemistry and processing have been paid attention to in many fields, in terms of reducing the consumption of resources and protecting the environment. Cellulose as an abundant biopolymer in nature, has been investigated for many years, due to its biodegradability, non-toxicity and thermal stability. (Klemm et al. 2005) These properties enable cellulose to have a great potential to be used as fuels, fibers, and packaging materials. However, the recalcitrant structure of cellulose, which results from a dense inter- and intra-molecular hydrogen bond network in combination with strong inter-sheet Van der Waals interactions, makes it difficult to dissolve and thus process cellulose. (Medronho, Science, and 2014 n.d.) Dissolving and processing cellulose in various solvent systems has been investigated during the last several decades. (S. Zhang et al. 2018a) (Michud et al. 2016) (S. Zhu et al. n.d.) (Feng and Chen 2008) Compared to the traditional, indirect and direct cellulose solvents, a certain class of ionic liquids are proved to be more environmentally friendly, because the processing conditions of cellulose are much milder, the solvent can be effectively recovered, and only small amounts of degradation products are generated from the solvent and solute. The cellulose shapes in the dissolved state are formed by spontaneous regeneration in a coagulation bath filled with a non-solvent such as water. The regenerated cellulose is easy to fabricate into the forms of films, textile fibers, hydrogels and sponges. (S. Wang et al. n.d.) Among these products, regenerated cellulose films possess similar properties regardless of the solvent systems. They commonly show high optical transmittance, excellent mechanical properties, and thermal stability. Several factors in the process have influences on the final product properties, which are the cellulose concentration, the presence of water molecules in the solutions, the solvent concentration and the temperature of the coagulation bath, as well as the drying temperature and humidity. (Liang et al. 2007) (Mazza et al. 2009) (Yang et al. 2012)

It has repeatedly been shown that a solution of a dissolving pulp (Enocell: birch prehydrolysis kraft) in 1,5-diazabicyclo [4.3.0] non-5-ene acetate ([DBNH][OAc]) was an appropriate system for dry-jet wet spinning of textile fibers, because the solutions revealed excellent spin stability and the final fibers presented superior tenacities and strength in the end. (Sixta et al. 2015a) (Michud et al. 2016) For this reason, it was then assumed that regenerated cellulose films could also be fabricated readily from this solvent system by casting and spinning. Meanwhile, the films were presumed to perform similar properties, which could be comparable with those regenerated from other solvent systems.

The aim of this thesis is to experimentally test this hypothesis. In this work experiments were conducted on casting and continuous spinning of Enocell/[DBNH][OAc] solutions. However, the dry-jet wet spinning of films with the flat nozzle was not successful, because the spinning equipment was not designed for it. Within the scope of the diploma thesis, it was not possible to retrofit the plant accordingly, therefore the obtained results of the continuous spinning tests were not fully discussed in this thesis. Furthermore, the optimum conditions during the processing of cellulose in [DBNH][OAc] were explored via changing the parameters, in order to produce regenerated films with high quality continuously in larger scale in the future.

1.2 Structure of the thesis

In chapter 2, the cellulose films regenerated from various solvents as well as the main properties of regenerated cellulose films (RCFs) were reviewed from the recent literatures. Particular emphasis was placed on the main characteristics of RCFs and on the process parameters that influence these properties. In chapter 3, the materials, procedures and characterization methods as well as the corresponding equations were demonstrated. Finally, the last section summarized the main findings, discussions and conclusions. The appendices listed the supplementary data, the few experimental trails on continuous dry-jet wet film spinning from cellulose/[DBNH]OAc.

2 Literature review

Cellulose is a linear biosynthesized polysaccharide with a repeating unit of glucose molecule. (French et al. 2017) These repeating units are linked by oxygen bridges formed through acetalization of two hydroxy groups at the C1 and C4 positions, as shown in Figure 1. Its degree of polymerization (the number of repeating units) depends on the original sources and the treatment methods of cellulose. (Pinkert et al. 2009a) (H. P. Fink et al. 2001) (Klemm et al. 2005) (Moon et al. 2011) The hydroxyl groups on its chains are in the equatorial direction, causing cellulose to be hydrophilic. (Medronho, Science, and 2014 n.d.) Due to a high number of hydroxy groups at the repeating units, a large quantity of intra- and inter-molecular hydrogen bonds exists within the cellulose chains (Figure 2), resulting in a high degree of crystallinity around 40-60%. Stable and stiff networks are therefore formed, leading to a very poor solubility of cellulose in most solvents, and difficulties in the processing of cellulose.

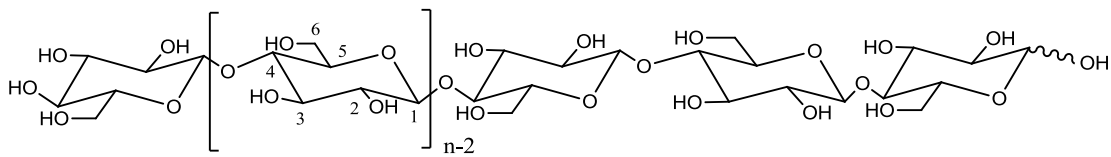


Figure 1. Molecular structure of a cellulose chain.

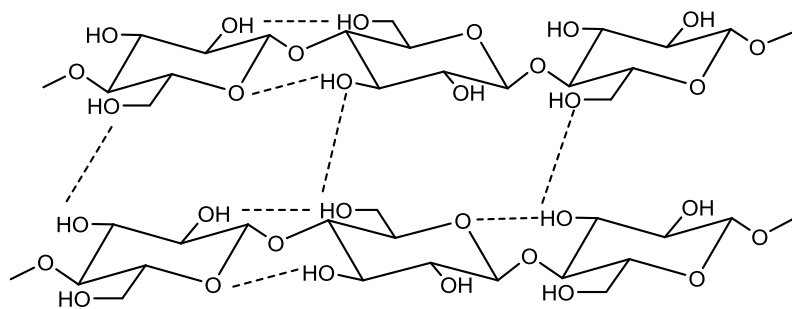


Figure 2. Intra- and inter- molecular hydrogen bonding in cellulose.

Nevertheless, many breakthroughs have been achieved in the industry in the processing and dissolving of cellulose. The Viscose technology has been a widely-used process to produce regenerated cellulose products from all kinds of cellulose resources for over 100 years.

(Heinze, Schwikal, and Barthel 2005) (Guidotti 2017) (Y. Xu, Lu, and Tang 2007) However, detrimental CS₂ and H₂S emissions which are released during the spinning process, as well as excessive water consumption renders this process not environmentally friendly. (Woodings and Textile Institute (Manchester 2001)) Thus, a viscose type of process called CarbaCell has been developed alternatively. Instead of xanthation, cellulose is converted to cellulose carbamate in this process. (H.-P. Fink, Ganster, and Lehmann 2014) However, this process is not yet commercialized most likely due to high costs and poor fiber properties.

Several other novel solvent systems for processing cellulose have been specifically developed to minimize the generation of hazardous byproducts. (Struszczyk et al. 1995) As a result, a Lyocell process using N-methylmorpholine-N-oxide monohydrate (NMMO) as a powerful direct cellulose solvent has been successfully developed and commercialized with the first installations in 1992 by Courtauld (Mobile, USA) and in 1997 by Lenzing AG. ("Process for the Preparation of Cellulose Sheet" 1994) The Lyocell process is an environmentally friendly process which consumes little amounts of fresh water while producing regenerated cellulose fibers with very high tensile strength especially under wet conditions (>31 cN/tex), but also under dry conditions (>37 cN/tex). A special feature of the NMMO-based Lyocell process is its very high solvent recovery of more than 99.5%, which renders the process environmentally very friendly. (Reddy and Yang 2015) (S. Zhang et al. 2018b) Apart from Lyocell fibers, this process can also produce regenerated cellulose films, gels and sponges. Nevertheless, some byproducts arise from side reactions of the solvent and the pulp, which affect the process behavior and can also lead to process instabilities. (Rosenau et al. 2001) Another classic process called Cuprammonium is to produce cupro-silk and cuprophane membranes, which are applied to hemodialysis treatment mostly. This process produces excellent products, but has impacts on environment on account of involving Cu(II) ions, so it is produced only by one company named Asahi Kasei. (Rodrigues Filho and Nascimento de Assunção 1993) However, recently, they expanded the production capacity to 17 kt/a owing to an increasing demand of specialty cellulose products.

In addition, a number of solvent systems such as ionic liquids have just been discovered and

only advanced in laboratory scale so far. This will be recounted in detail in the following sections.

2.1 Cellulose solvents

Two categories of systems can be applied for cellulose dissolution, derivatizing or non-derivatizing, depending on their interactions with the cellulose chains. (Medronho, Science, and 2014 n.d.) The former type usually induces covalent modifications on cellulose backbones via functionalization of the hydroxyl groups, so that hydrogen bonds can be broken. (Sen, Martin, and Argyropoulos 2013) The NaOH/ C₂S solvent system for the Viscose process mentioned above is a typical derivatizing solvent. It generally involves a high content of water to carry agents for an adequate cellulose dissolution in derivatizing solvent systems. However, with the presence of water, more side reactions would be promoted. (Pinkert et al. 2009a) In contrast, non-derivatizing solvents, for instance, inorganic molten salt hydrates and transition metal complexes, are capable of dissolving cellulose via separating the individual cellulose chains from each other without chemical modification. Dimethylacetamide/LiCl, NaOH/urea/water, N-methylmorpholine oxide (NMMO)/water and ionic liquids, to name the most important ones, are non-derivatizing solvents. (McCormick and Callais 1987) (Shengdong Zhu et al. 2006) (Pinkert et al. 2009b) (S. Zhang et al. 2018a)

Commonly, several opinions are widely accepted to describe cellulose dissolution. (L Schulz et al. n.d.) (Sen, Martin, and Argyropoulos 2013) Structurally, cellulose chains are swollen in solvents before forming a colloidal-state or a dissolved-state network. According to Liane Schulz, aggregations and associations of cellulose chains still exist in the solvents, even though the cellulose is already dissolved on a macro level. (Liane Schulz, Seger, and Burchard 2000) In the systems based on aqueous NaOH, hydrates are formed in combination with water, which enable inter- and intra- molecular hydrogen bonds between cellulose chains to cleavage. For NMMO-based solvents, it was widely-accepted that the polar N-O group could break intermolecular cellulosic hydrogen bonds readily and then two new

hydrogen bonds are formed with the cellulose hydroxyl groups. (H. Wang, Gurau, and Rogers 2012) In contrast, the mechanism of cellulose dissolution in LiCl/DMAc (inorganic/organic) was considered different due to the basicity of Cl^- and its accumulation along the cellulose chains causing chain separation because of charge repulsion. (Dawsey and McCormick 1990)

2.2 Ionic liquids

Compared to classic solvent systems, some of the ionic liquids are considered promising solvents for cellulose. Ionic liquids are regarded as environmentally friendly because of their non-volatility, which is often not totally true. Only a few ionic liquids are non-toxic and allow complete recovery in a closed-loop operation. (S Zhu et al. n.d.) (Fort et al. n.d.) Special anion-cation combinations allow cellulose to dissolve in high concentrations. The high basicity of the anion causes the formation of pronounced hydrogen bonds with the OH-groups of cellulose, while the cation interacts with the hydrophobic part of the cellulose, thus expanding and solvating the stacked layers. A short overview of currently accepted mechanisms of cellulose dissolution is given below.

Many ionic liquids have been studied with regard to their cellulose dissolution capacities. (Saha et al. 2003) (Hao Zhang et al. 2005) (Laus et al. 2005) (Kilpeläinen et al. 2007) As mentioned above, cellulose dissolution is governed by both cations and anions, although it is not totally clear which of them impacts principally. (Heinze, Schwikal, and Barthel 2005) It is popularly accepted that anions act as hydrogen bond acceptors, and cations act as donors. A complex containing donor and acceptor is formed to disrupt the original hydrogen bonds of cellulose chains and to form the new ones. (Pinkert et al. 2009c) Therefore, the anions with higher hydrogen bond basicity and dipolarity provide a higher capacity to dissolve cellulose. For some systems, the dissolution is mainly dominated by interactions of IL anions and the hydroxyl groups of cellulose chains. (Fukaya et al. 2008) (J. Zhang et al. 2010) (Pu, Jiang, and Ragauskas 2007) However, on the other hand, the ability of a cation to donate hydrogen bonds is influenced by the acceptor, so the choice of cations is also important.

(Wanasekara et al. 2016a) Cations containing methylimidazolium and methylpyridinium cores along with allyl chains have been proven to be the most efficient ones, since they function as the shield of anions and cellulose complexes. Furthermore, the longer the side chains of the cations are, the lower solvent power the ILs have, because of the reduced effective anion concentration. The more asymmetric the cations are, the lower the melting point is. (Remsing et al. 2006) The most effective anions with the highest hydrogen bond basicity are chloride, acetate, formate and other carboxylates with an electron-donating substituent X in the [XCOO] groups. (A. Xu, Chen, and Wang 2018) They are used in combination with imidazolium or superbase-based cations to form efficient cellulose solvents such as [bmim]Cl, [amim]Cl, [DBNH][OAc] and [DBNH][CO₂Et]. (Rodrigues Filho and Nascimento de Assunção 1993) (H. Wang, Gurau, and Rogers 2012)

2.2.1 [DBNH][OAc]

1,5-diazabicyclo [4.3.0] non-5-ene acetate ([DBNH]OAc) is a novel protic ionic liquid (PIL) system with a low melting point for direct cellulose dissolution. [DBNH]OAc contains superbase and acid ion pairs. The solutions of cellulose and [DBNH]OAc have been proven to have the outstanding flowability for spinning. The spun fibers usually present excellent properties. (Michud et al. 2016) (Hummel et al. 2015) (Sixta et al. 2015b) Hauru et al. have researched and compared spinnability of the solutions of cellulose dissolved in [emim]OAc, [DBNH]OAc and NMMO. The results showed that the solutions of cellulose dissolved in [DBNH]OAc and NMMO could be spun even with very high draw ratio. (L. Hauru et al. n.d.) (Wanasekara et al. 2016a) Nevertheless, the price of DBN-based ILs is still very high because of their low production, which increases the production costs of regenerated cellulose from DBN-based ILs.

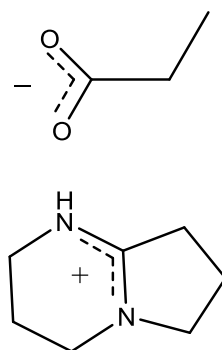


Figure 3. Chemical structure of [DBNH]OAc.

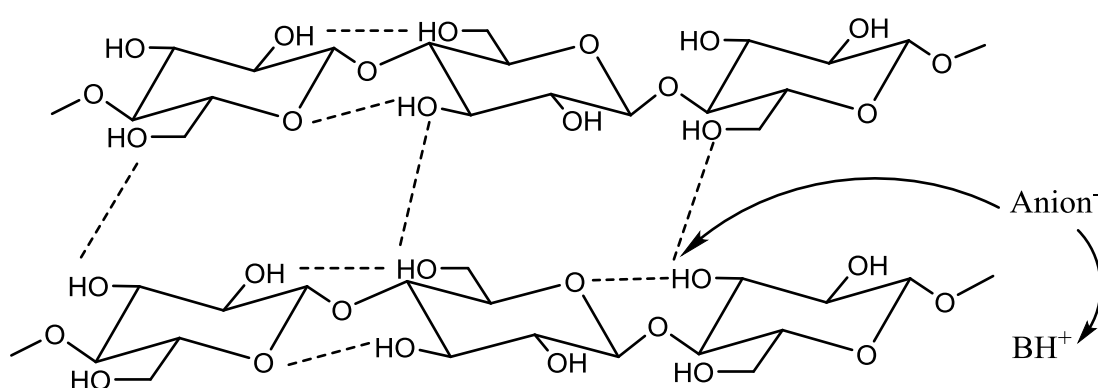


Figure 4. Dissolution mechanism of cellulose in [DBNH]OAc

The mechanism of dissolving cellulose in [DBNH]OAc was sketched in Figure 4. It presumes that no extended hydrogen bonds are formed between the ion pairs of [DBNH]OAc. It is between carboxylate oxygen atoms and N1 atoms of [DBNH]OAc that strong hydrogen bonds are formed. (Parviainen et al. n.d.) Thereby, a proton from a hydroxyl group of cellulose is split off from the anion in order to break the hydrogen bond.

2.3 Regenerated cellulose materials

In commercial processes, the filtered solution is spun into fibers or filaments via a wet or dry-jet wet spinning process. Besides, a coagulation bath and a washing bath are always required to regenerate cellulose and to wash away the solvents respectively. (Woodings and Textile Institute (Manchester 2001) (H. P. Fink et al. 2001) The cellulose regeneration is a

physical process of solvent and non-solvent exchange. Non-solvent refers to the coagulant that poorly dissolves cellulose and serves as a medium to convert native cellulose into a state with certain shapes. During coagulation, the non-solvent penetrates the gel-like cellulose and the solvent diffuses out of it. Hydrogen bonds formed between the solvent and cellulose chains are disrupted, and a new cellulose network is reformed through the aggregation of new hydrogen bonds between and within cellulose chains. (Pang et al. 2015) (S. Wang et al. n.d.) Thus, the final properties of cellulose materials are influenced by the non-solvent in the coagulation bath, the immersion time in the coagulation media and the temperature of the bath. The more detailed effects are discussed in the following sections.

2.3.1 Regenerated cellulose films and membranes

Thin films (cellophane and cuprophane) with high optical transmittance can be fabricated by the Viscose process and the Cuprammonium process, based on an extrusion technology. The dope is extruded from wide nozzle slits and further is coagulated in a form of ribbon. The ribbon is then stretched and sized by consecutive rollers. (H. P. Fink et al. 2001) Another technique to form regenerated cellulose films developed by Fink et al. is the blown-film manufacturing process. (H.-P. Fink, Weigel, and Bohn 1999) (H.-P. Fink, Ganster, and Lehmann 2014) It is a simpler and more cost-effective process, in which it is easier to control film properties. The cellulose solution in molten state is extruded through a circular blow nozzle with a fixed diameter. In the center of the ring nozzle, there are several air suppliers to blow up the film transversely. The blowing procedure should be carried out before the melt enters into a coagulation bath containing an anti-solvent. The non-solvents of the precipitation bath can be differential to obtain the desired inner and outer surface. In sequence, the films are folded and transported by deflection rollers for further washing, post-treatment and drying. The films produced by the blown-film process are thinner and more homogeneous, because of being orientated in each direction by stretch. Beyond this process, casting is commonly used on a lab scale, since it is extraordinary simple and time-saving for a small scale. Moreover, various substrates can be chosen for casting, such as glass, metal,

PMMA plates, as long as the plate is flat and strong enough to fix the films. (Wawro, Hummel, et al. n.d.) (Lina Zhang, Dong Ruan, and Zhou 2001).

Main properties of regenerated cellulose films

When a solution of cellulose is immersed in a non-solvent of the coagulation bath, cellulose molecular chains are re-entangled and a cellulose gel with tiny pores is reprecipitated. During drying, water and non-solvent are evaporated and the pores partially collapse into a regenerated cellulose film with a dense structure. Such structures result in excellent properties of regenerated cellulose films, which are described in detail below.

Optical properties. Generally, transparent or hemi-transparent cellulose films can be produced from the solvent systems. The optical transmittance can reach 90% in the visible region and over 70% in the ultraviolet region, when using UV-visible spectroscopy to investigate RCFs. (Yang et al. 2011a) (Lina Zhang, Dong Ruan, and Zhou 2001) (S. Zhang et al. 2018b) Based on XRD measurements, it is found that fewer aggregates are contained in such regenerated cellulose films. As a result, RCFs scatter less light. (Yang et al. 2011b)

Mechanical properties. It is well known that the stretched films present a high tensile strength and Young's Modulus resulting from orientated macromolecules. However, the regenerated cellulose films without stretch can present excellent mechanical properties as well. Appendix 1 lists the mechanical properties of the regenerated cellulose films fabricated from different solvent systems by casting. They therefore have a great potential for the packaging of food, drugs and cosmetics.

Oxygen and water vapor permeability. For packaging applications, it is vital to investigate the oxygen and water vapor permeability of the regenerated cellulose films. Due to the high hydrophilicity of cellulose, regenerated cellulose films are usually water-vapor-permeable. Moreover, porous structures of cellulose films resulting from solvent and non-solvent

exchange would reduce their barrier properties further. However, Isogai et al. have produced a regenerated cellulose film with high oxygen barrier properties from the NaOH/urea system. The lowest value was around $0.003 \text{ mL} \cdot \mu\text{m} \cdot \text{m}^{-1} \cdot \text{day}^{-1} \cdot \text{kPa}^{-1}$ (0% relative humidity). This high barrier properties confirmed that regenerated cellulose films could be an oxygen barrier, when using an appropriate coagulation condition and drying method. (Yang et al. 2011a) Based on their research results, the denser a film is, the lower its oxygen and water vapor permeability are, and the better its barrier properties are. J. Wang et al. have summarized the barrier classifications of films in terms of oxygen and water vapor permeability, as well as their possible applications in Table 1. (J. Wang et al. 2018)

Table 1. Barrier classifications of films in terms of oxygen and water vapor permeability.

Grade	Oxygen permeability $\text{cm}^3 \cdot \mu\text{m}/\text{m}^2 \cdot \text{day} \cdot \text{atm}$	Water vapor permeability $\text{g} \cdot \mu\text{m}/\text{m}^2 \cdot \text{day} \cdot \text{kPa}$	Applications
High	40-400	40-400	Fruits, vegetable, salads casing; Meat packaging
Medium	400-4000	400-1000	Fruits, vegetable, salads casing; Cheese
Low	4000-40000	1000-3000	Bakery
Poor	>40000	>3000	Bakery

Factors influencing the properties of regenerated cellulose films

Solution parameters. The mechanical properties depend to a high extent on the cellulose concentration in the solutions. (Wawro, Stęplewski, et al. n.d.) (S. Liu and Zhang 2009) (Z. Liu et al. 2011) Under the same processing and post-treatment conditions, an optimum concentration (or range) of cellulose usually exists. With an increasing cellulose concentration in the solution, the elongation at break of regenerated cellulose films increases. Besides, the films with a higher concentration are less oxygen permeable, because denser films can be produced from it.

Coagulation bath. Regenerated cellulose films have a different morphology in coagulation baths with different non-solvents and at different temperatures, since the macroscopic morphology of regenerated cellulose depends on how cellulose/IL solution interacts with the regeneration solvent. (H. Wang, Gurau, and Rogers 2012) Moreover, the two surfaces of the cast films after coagulation are different from each other. In the NaOH/Urea solvent system, the neutralization of alkali with aqueous sulfuric acid as coagulation medium leaves homogeneous porous structures, which reduces the optical transmittance value. (Li et al. n.d.) Zhang et al. have explored water, methanol, ethanol and acetone as coagulation media for regenerated cellulose films from a LiCl–DMAc solvent system. (Lina Zhang et al. 2005) Acetone has been proven to be a better coagulation medium to obtain an amorphous cellulose structure with high optical transmittance. (Cai et al. 2010) Furthermore, the stronger a coagulant is, the faster the coagulation rate is, so that cellulose chains are unable to pack in time, resulting in the lower crystallinity of the product. Studies made by Yang et al. shows that the films are in different densities with different non-solvents and temperatures of the coagulation bath. Besides, the films coagulated in ethanol at 0 °C gives a lower oxygen permeability, compared to those coagulated in aqueous sulfuric acid and sodium sulfide. The higher the temperature of the precipitation bath is, the more likely to form a robust network. This leads to a denser film with higher barrier properties and better mechanical properties. (Yang et al. 2011a) In the casting process, the surface in contact with the non-solvent or coagulant is usually not as smooth as the opposite surface. In the blown-film process, the different precipitation media of inner and outer sides also induce an asymmetrical morphology.

Drying conditions. Several drying methods aim at optimizing the mechanical properties of the regenerated cellulose films, such as vacuum oven drying, freeze drying, controlled humidity and temperature drying, as well as hot-press drying. (Yang et al. 2011a) Press-vacuum has been proven to be an effective method to dry regenerated cellulose films, as the films have the highest density, crystallinity, tensile strength and Young's Modulus as well as a lower oxygen permeability.

2.3.2 Regenerated cellulose fibers

Regenerated cellulose fibers are the most important products from ionic liquids in the application of textile and garments. Apart from the traditional Viscose fibers, the development of NMMO-based regenerated cellulose fibers have been made to obtain the fibers with both low titer and high strength. (Wanasekara et al. 2016a) Rheological properties are crucial for the regeneration of cellulose fibers, as they influence the spinnability of solutions, which has a direct effect on the final fiber properties and yields. (L. Hauru et al. n.d.) (Wanasekara et al. 2016b)

2.3.3 Other regenerated cellulose materials

Regenerated cellulose materials can be formed to other shapes, for example hydrogels, aerogels, sponges and beads. (Chang and Zhang 2011) In the cellulose hydrogels, cross-linked or aggregated networks can be obtained to retain water. Hydrogels and aerogels with a macroporous structure can be produced by coagulation in a water bath and heating- or freeze- drying. (Gan et al. 2017) The advantages of biocompatibility, biodegradability and hydrophilicity improve their potentials to be applied in biomedical and pharmaceutical fields. (Kimura et al. 2015)

2.4 Modification of regenerated cellulose films

For the packaging applications, it is imperative that RCFs are of high quality, with a combination of high tensile strength, high Young's Modulus, thermal stability, and better barrier properties, especially for food casing. Plasticizing, blending with additives like cellulose whiskers or pectin and other treatment methods during precipitation, such as pre-gelation were studied to improve the properties of regenerated cellulose films. (Qi, Chang, and Zhang 2009) (H.-P. Fink, Ganster, and Lehmann 2014) (Liang et al. 2007) Betulin as a naturally hydrophobic chemical was used for the coating of regenerated cellulose fabrics. It significantly improves water repellency and hydrophobicity of regenerated cellulose fibers and films. (Huang, Li, and Ek 2018)

3. Materials and methods

In this chapter, the materials and the equipment used in the experiments were discussed in chapter 3.1. The characterization methods of regenerated cellulose films were demonstrated in chapter 3.2, including the equations involved into the calculations.

3.1 Materials

Birch prehydrolyzed kraft (PHK) dissolving pulp, further referred to as Enocell pulp in the following sections, was supplied in the form of pulp sheets by Stora Enso, Finland, and ground by a Wiley mill.

1,5-diazabicyclo [4.3.0] non-5-ene (99% Fluorochem, UK) and acetic acid (100% Merck, Germany) were used to prepare 1,5-diazabicyclo [4.3.0] non-5-ene acetate ([DBNH]OAc) for the dissolution of cellulose. An equimolar amount of acetate acid was added slowly to DBN while the system was cooled actively by a temperature controller.

Ethanol (94 V%, CAS: 64-17-5, Altia Oy) and deionized water were used as a coagulation bath and a washing bath respectively. High purity Betulin was purchased from Innomost, Finland, to mix with Enocell pulp in [DBNH]OAc as a hydrophobic agent. It is a white powder, isolated from wild Finnish birch bark. It is insoluble in water but soluble in ethanol of 0.7 wt%.

Cellophane (P25 Innovia Films, UK) was received from a partner lab (Mines ParisTech, France) as a reference. It was produced by the Viscose process.

3.2 Methods

3.2.1 Dissolution of cellulose

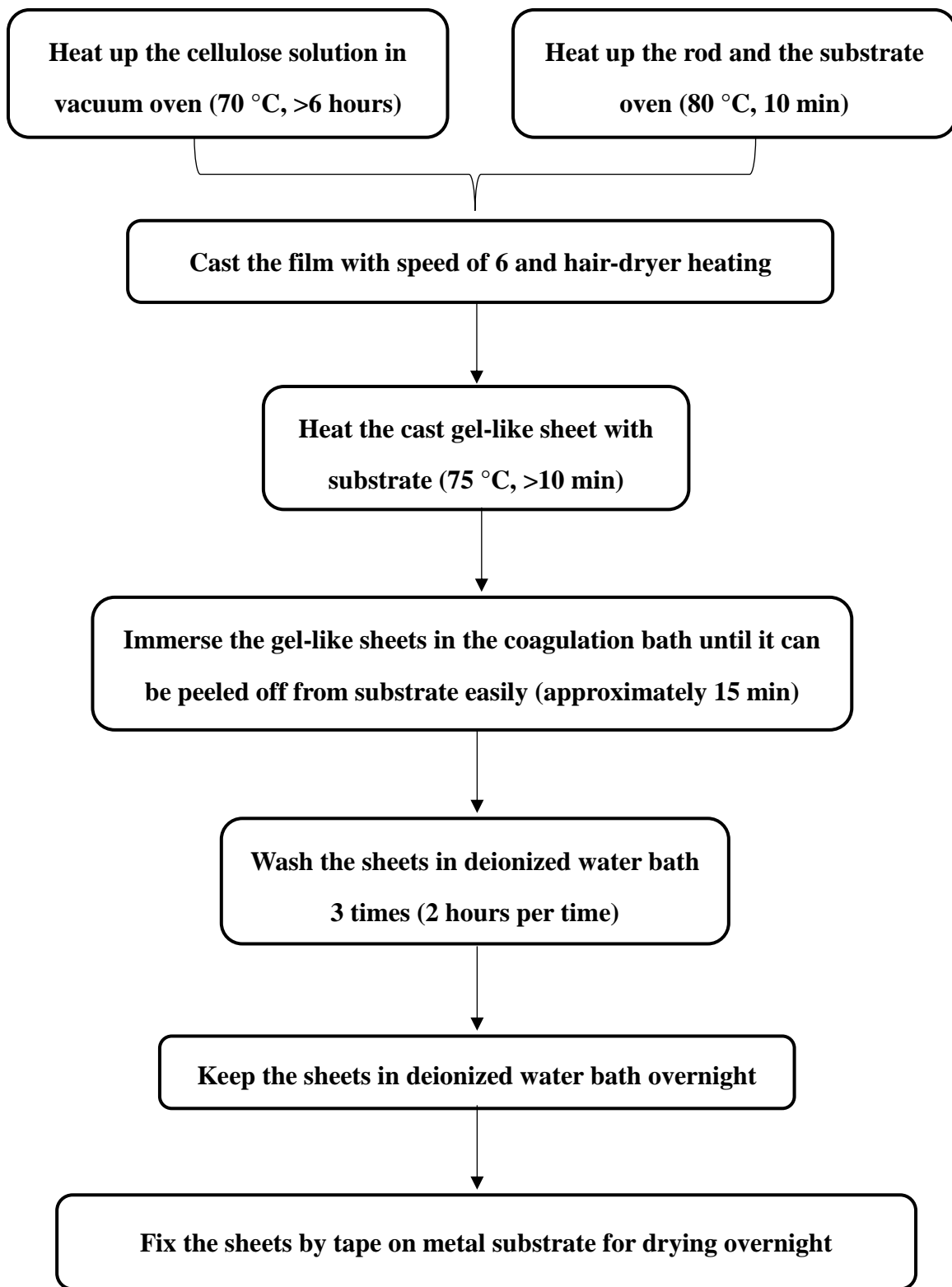
The synthesized and solidified [DBNH]OAc was melted at 75 °C in a water bath and mixed with different concentrations of Enocell pulp (4, 5, 4.7, 5.2, 5.4, 5.6, 5.8 and 6 wt%) in a vertical kneader described in our previous articles. (Sixta et al. 2015c) (Ma et al. 2018) The mixture was stirred vigorously for 2 minutes before dissolution at 80 °C and 30 rpm for 90 minutes.

The concentration of Betulin was 10 wt%. It was based on the weight of Enocell pulp. Betulin was pre-mixed with [DBNH]OAc for 2.5 hours, and Enocell pulp was then added into the mixture to blend for another 1.5 hours. The dissolved cellulose in [DBNH]OAc was in a gel state and was then transferred into glass bottles with lids. Before casting films, the bottles of solutions were kept in a vacuum oven under 75 °C at least for 6 hours to remove all the air bubbles.

3.2.2 Preparation of regenerated cellulose films

The film casting was conducted with a K-rod coater (K202 Control coater), whereby and the thickness of the films was determined by the rod with a diameter of 500 µm and a casting speed of 6. The solution was poured slowly onto a substrate. The rod and the substrate were also heated up in the oven to 80 °C beforehand. Glass plates (20x20 cm, Silicagel 60 F GLP), PMMA plates and metal plates were applied as the substrates. The films were in a solution state after casting. They were then preserved in an oven at 80 °C for at least 10 minutes to cure possible defaults directly. The solutions on the substrates were moved to a coagulation bath for precipitation afterwards. The anti-solvents of the regeneration bath were varied: pure EtOH and two different aqueous EtOH. The ratios of EtOH and deionized water were 4:1 and 1:1 respectively. Some of the films were also coagulated in open air to compare the final properties of the films. The time of immersion depended on the individual film. It was sufficient as long as the gel-state-film could be separated from the substrate. The films in the sheet form were immersed in deionized water and washed thoroughly. The films were fixed with a tape onto a flat metal or glass substrate for drying overnight afterwards. The

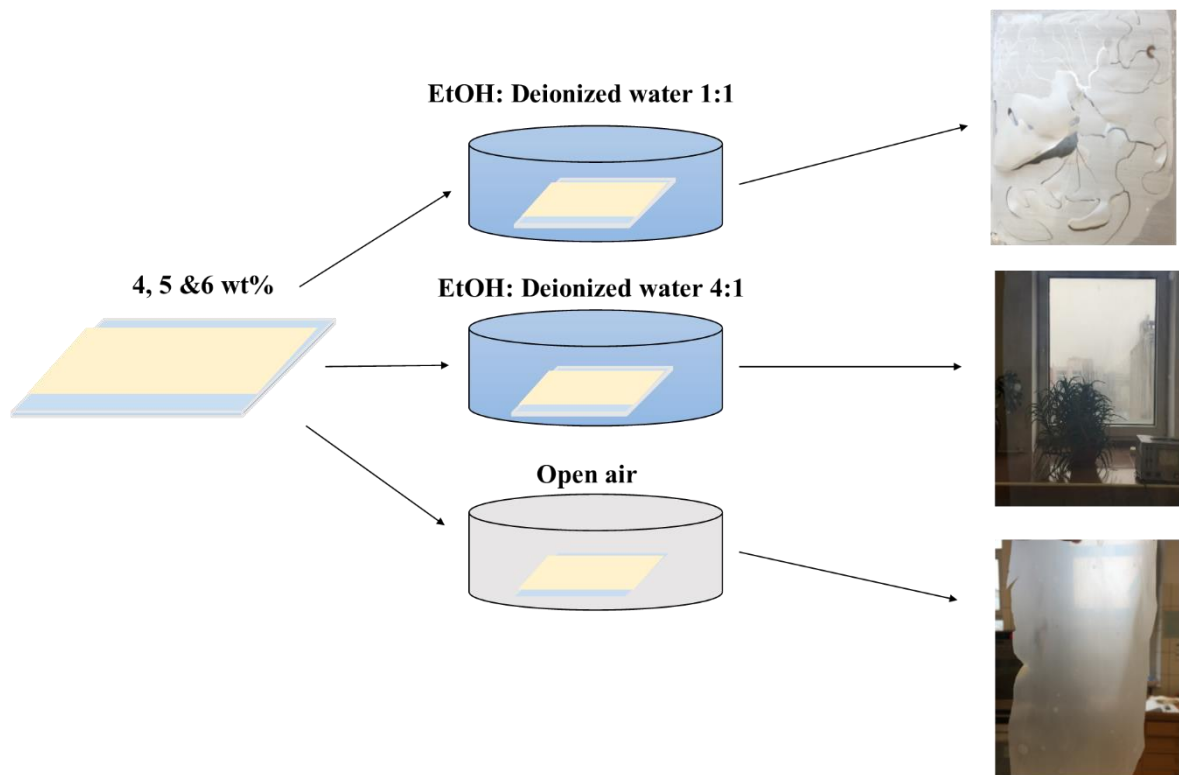
conditions were varied including drying in a freeze dryer and a moisture cabinet. The moisture cabinet enabled to change and control the temperature and humidity at the same time. Constant humidity and reduced humidity were used, including constant 50% RH and 23 °C, constant 50% RH and 50 °C, constant 30% RH and 23 °C, as well as reduced humidity from 95% RH to 55% RH and 23 °C. Among the films, those containing 4, 5 and 6 wt% of cellulose were cast in the Institute of Biopolymers and Chemical Fibers in Poland. Figure 5 illustrates the protocol of casting films. The illustrations in Figure 6 display in more detail of the procedure of casting the regenerated cellulose films with varied parameters.



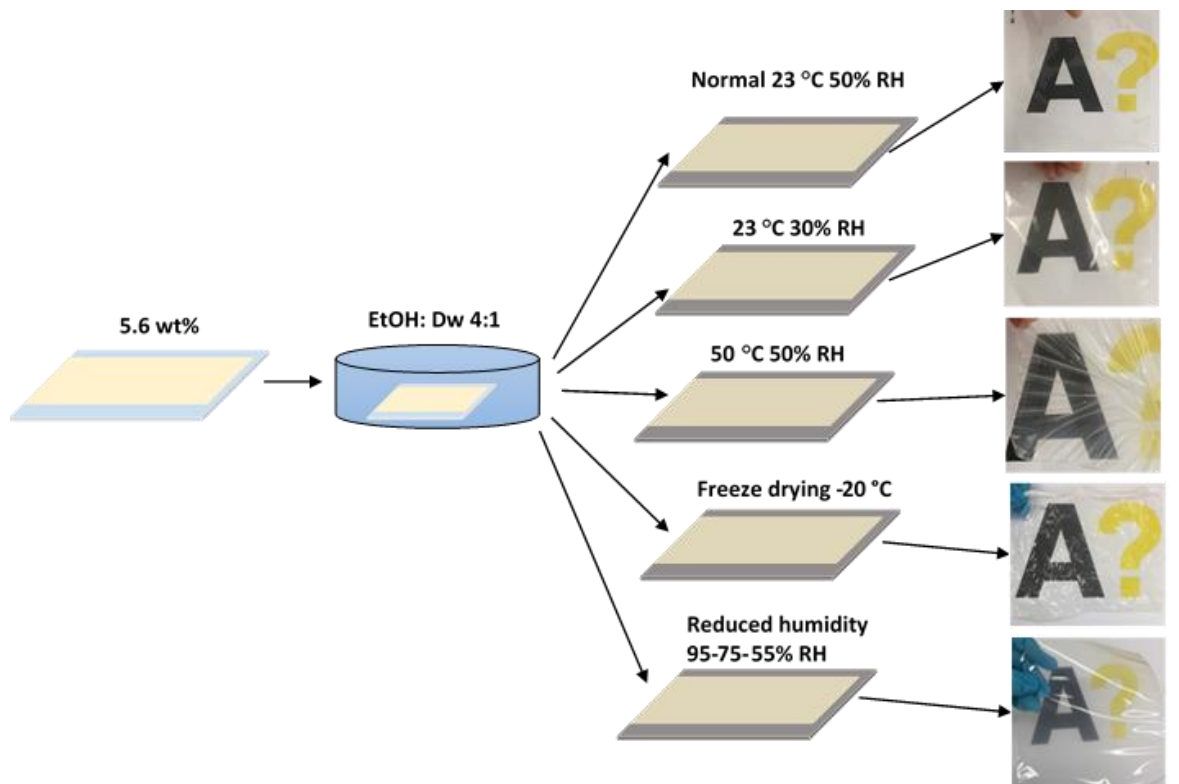
(a)

Figure 5. Illustration of the protocol of casting regenerated cellulose films.

(a) Different coagulation baths



(b) Different drying methods



(c) Addition of Betulin

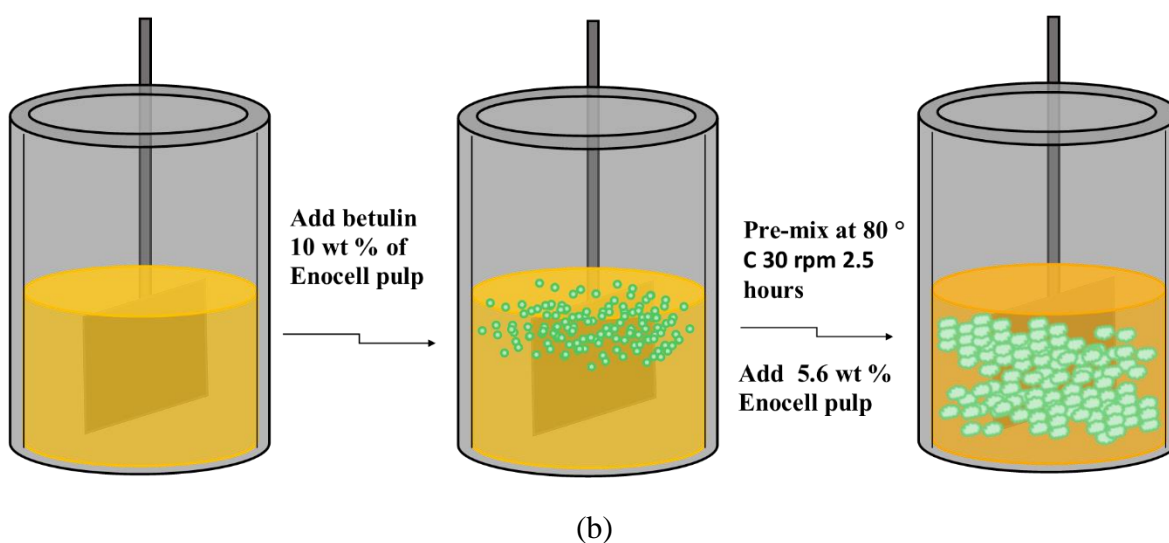


Figure 6. Illustrations of the procedure of casting regenerated cellulose films with various parameters: (a) coagulation media; (b) drying conditions; (c) with the addition of Betulin by blending.

3.3 Characterizations

Basic properties. The thickness of the films was determined by a micrometer (L&W SE 250D) according to the standard ISO 527-3:1995.

Degree of polymerization of original pulp and regenerated films. The degree of polymerization (DP) of the original pulp and the regenerated cellulose films were measured by an Ubbelohde viscometer, according to the standard method SCAN-CM 15:88. The original pulp and the regenerated cellulose films were ground into powders and dissolved in a cupri-ethylenediamine (CED) solution. Before applying suction, the bottles with samples were kept in a water bath at 25 °C for 40 minutes. The time that the solution required to pass through the two marks of Ubbelohde viscometer was recorded at least for 3 times of each sample. In order to ensure the reliability of the results, the difference between each result was less than 0.3s. The viscosity-average value was then calculated according to the

equations (1)-(3). The corresponding value of $[\eta] \cdot c$ can be looked up in the table $[\eta] \cdot c$ at different values of the viscosity ratio in the standard method SCAN-CM 15:88.

$$\eta_{rel} = h \cdot t_n \quad (1)$$

$$[\eta] = \lim_{c \rightarrow 0} \frac{\eta - \eta_0}{\eta_0 \cdot c} \quad (2)$$

$$c = \frac{\text{Sample weight}}{\text{Dry matter content}} \quad (3)$$

The molecular mass distribution of cellulose. The molecular mass distribution (MMD) of cellulose was determined by gel permeation chromatography (GPC) Ultimate 3000. A pre-column, four analytical columns and a RI-detector were consisted of in this GPC system. The ground samples were activated with 4.0 mL of MilliQ-water, 4.0 mL of acetone and 4.0mL of DMAc in tubes with vacuum manifold subsequently, followed by the dissolution in 5.0 mL of 90 g/L LiCl/DMAc. The sample concentration of 1.0 mg/mL and LiCl concentration of 9 g/L was ready for analysis then. The samples were filtrated with 0.2 μm syringe filter. The measurement was then carried out that a volume of 100 μl solution was separated at 25 °C at a flow rate of 0.750 ml/min with 9 g/l LiCl/DMAc. The results of the molar mass distribution were corrected with direct-standard-calibration. (Berggren et al. 2003) (Michud, Hummel, and Sixta 2015)

Rheological measurements Rheological properties of cellulose solutions were detected under dynamic oscillatory shear via a rheometer with a 50 mm parallel-plate geometry (Anton paar MCR-301). The shear rate range was between 0.01 and 100 s^{-1} and frequency range was from 0.1 to 100 Hz. The temperature was from 50 °C to 100 °C. (L. K. J. Hauru et al. 2014)

Scanning electron microscopy (SEM) SEM images were captured via Zeiss Sigma VP with an accelerating voltage of 2.5 kV. The regenerated cellulose films were fixed with a carbon tape on holders. For cross-section observation, the films were broken according to the cryo-fracture method. Then the surfaces were coated with platinum (90 seconds) before making observations.

Mechanical properties Tensile strength, elongation at break and Young's modulus of the regenerated films were determined by MTS 400 M tensile and compression tester, equipped with a 100N load cell at a rate of 10 mm/min, according to ISO 527-3:1995. The films were cut by a scalpel into specimens. The width of the specimen was 15mm and the gauge length was 50 mm. Before testing, the specimens were kept in the conditioning room under 50% RH and 23 °C for overnight.

Thermogravimetric analysis (TGA) The thermal stability of the original Enocell pulp and the regenerated cellulose films was determined by TA Instruments Q500. The regenerated cellulose films were cut into pieces and dried at 80 °C beforehand. Approximately 5mg of sample were well placed in a platinum pan for each measurement. The temperature increased 20 °C per minute from 30 °C to 500 °C. N₂ was used to purge the chamber during the measurement.

Transparency The optical transmittances of the regenerated films were measured from 400 to 900 nm by using a Shimadzu UV-1700 UV-V spectrophotometer.

Water vapor permeability Water vapor permeability of RCF containing with and without Betulin was determined with a gravimetric cup method at University of Helsinki. The measurement was conducted under 23 °C and 73% RH as the standard E 96/E 96 M describes. Dried sodium chloride grains as a water adsorption agent were put in an aluminum dish. The weight of the films including the cups were measured and recorded at least every 6 hours. In the meantime, the humidity and temperature of the sealed containers were placed in and were measured. Firstly, a graph of the relationship between the time and the changes in mass of the cups was plotted. Based on this graph, the slope of the weight of water vapor that passed through the films and the time was determined. WVTR and WVP were then calculated according to equations (4) and (5). (J. Wang et al. 2018)

$$WVTR = \frac{\text{Weight passed through from the film}}{\text{area} \times \text{time}} \text{ g} \cdot \text{m}^{-2} \cdot \text{day}^{-1} \quad (4)$$

$$WVP = \frac{WVTR \times \text{thickness}}{\text{saturated press} \cdot \Delta\%RH} \text{ g} \cdot \mu\text{m} \cdot \text{m}^{-2} \cdot \text{day}^{-1} \cdot \text{kPa}^{-1} \quad (5)$$

Water contact angle Contact angles of the films with and without the addition of Betulin were measured via a Contact Angle Meter CAM 200, by taking photos of the water droplets on the films. Three points were measured per type of the films to average the values. This analysis was to check the influence of the hydrophobic agent Betulin on the hydrophilicity.

Elemental analysis The efficiency of washing away the [DBNH]OAc from the regenerated films by deionized water was assessed based on the amount of nitrogen left in the films. The elemental analysis was determined by an elemental analyzer (Perkin Elmer 2400 CHNS/O Analyzer).

4 Results and discussion

In this chapter the main results were demonstrated together with an interpretation of the images and figures.

4.1 Influence of the cellulose concentration and the coagulation bath composition on the film properties

The solutions with 4, 5 and 6 wt% Enocell were firstly casted to compare the differences. As shown in Figure 6 (a), the films were thinner with 4wt% of pulp, but at the same time brittle and shrunk extensively compared to those with 6wt% of pulp. None of these films, specimen for tensile testing could be prepared. Only at a concentration of 5 wt%, the dried films were transparent, and strong enough. From this it was derived that the optimum concentration for casting films from [DBNH]OAc/cellulose solution should be between 5 to 6 wt%.

Meanwhile, according to Figure 6 (a), the appearance of the films was strongly dependent on the coagulated conditions. The films coagulated in aqueous ethanol (1:1) shrunk drastically with the presence of large opaque areas. However, a coagulation bath with an ethanol-to-water ration(v) of 4:1 brought high transparency and an acceptable strength to the films. When coagulating the dope in the open air, the films were whiteish and opaque. Since the ionic liquid diffused out of the gel-state sheet faster in an aqueous non-solvent than in the air, there was presumably no enough time for hydrogen bonds to rearrange when being coagulated in aqueous ethanol.

4.2 The rheological properties of cellulose/[DBNH]OAc solutions

4.2.1 Steady shear viscosity

The complex viscosity of each solution at 80 °C was plotted as a function of the angular frequency in Figure 7. It showed that all the solutions of Enocell/[DBNH]OAc performed shear-thinning behavior with the increased shear rates. As it was demonstrated in chapter 2.1, some entangled cellulose chains were still contained in the solution, although cellulose was dissolved on a macro level. Hence when cellulose/[DBNH]OAc solution was exposed to high shear rates, some of the macromolecule entanglements were untangled, which increased its fluidity and thus decreased its viscosity. Moreover, it was also found that the higher the cellulose concentration was, the higher the complex viscosity was. As soon as Betulin was mixed into the solution, the complex viscosity increased by 1000 times. This might be due to the rigid triterpene groups of Betulin molecules, and the aggregates of Betulin due to the poor solubility of Betulin in ionic liquid. (Huang, Li, and Ek 2018) This observation was logical and reasonable, as the solution structure was more complicated with more entanglements and desolvation molecules. (Chen et al. 2011)

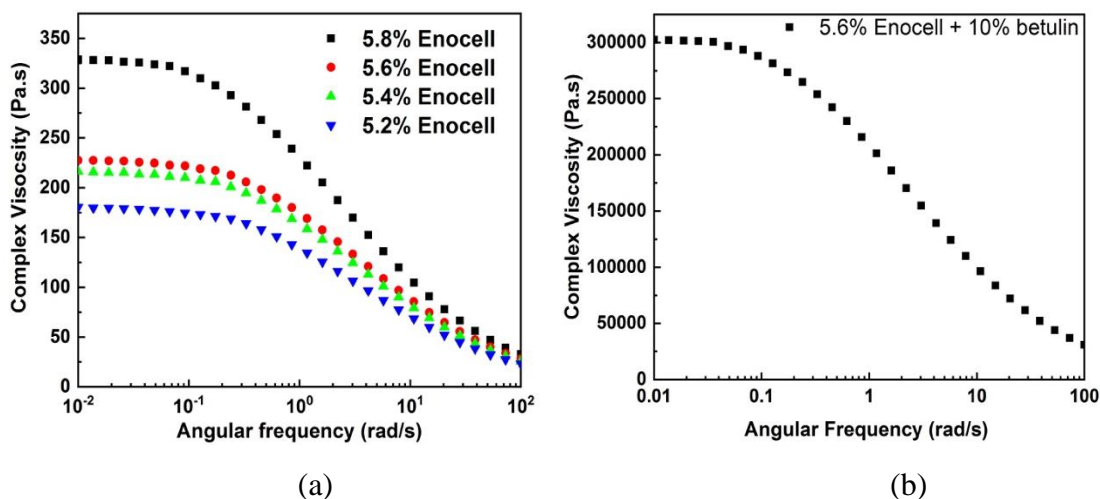


Figure 7. Complex viscosity as a function of angular frequency, for cellulose/[DBNH]OAc solutions at 80 °C (a) with different concentrations of Enocell and (b) with addition of Betulin.

4.2.2 Storage modulus and loss modulus

As expected, the dynamic modulus varied slightly with the increase of the concentration of

Enocell in the solutions, as presented in Figure 8(a). The cross-over (COP) of the storage modulus (G') and the loss modulus (G'') grew in when the concentration increased. The solution behaved more like an elastic solid with a widened elastic region, because the cellulose chains were closer to each other in the solutions with higher concentrations. (Sammons et al. 2008) However with 10 wt% Betulin inside, the cross-over point of storage and loss modulus did not occur between the frequency of 0.01 to 100 s^{-1} , due to the insoluble aggregates of Betulin.

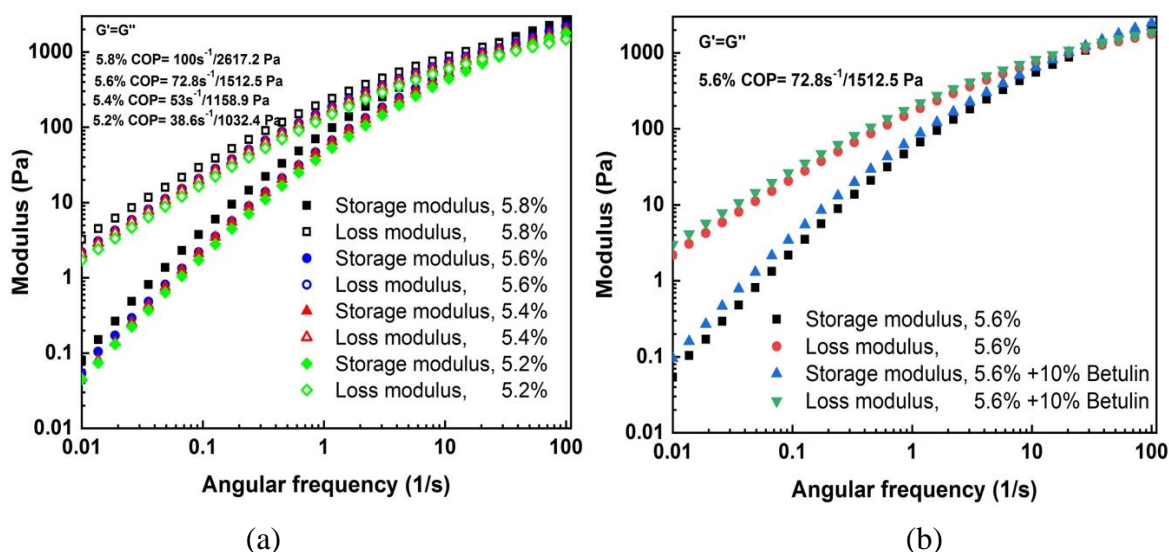


Figure 8. The storage modulus and loss modulus of cellulose/[DBNH]OAc (a) with different concentrations at 80 °C, and (b) containing with Betulin.

4.3 Characterization of regenerated cellulose films

4.3.1 MMD and Degree of polymerization

It was observed that the shape of the MMD curves of the regenerated films did not deviate significantly from the original cellulose materials, regardless of the Enocell concentration, drying methods and the addition of a hydrophobic agent, as shown in Figure 9. Since [DBNH]OAc dissolved cellulose under significantly milder conditions (lower temperature) than imidazolium-based ionic liquids with a chloride anion ([bmim]Cl and [amim]Cl), hardly any cellulose degradation occurs in contrast to the solution in latter solvents. Figure 10 compared the viscosimetric DP_v of the original cellulose with that of the regenerated

films. A moderate drop of the DPv after the dissolution and the regeneration of cellulose indicated that dissolution and processing in [DBNH]OAc caused only a slight degradation of cellulose. Meanwhile, the coagulation medium showed to affect the DPv of the regenerated films. Coagulation in the open air induced a slight decrease of DPv, compared to coagulation in aqueous ethanol. This might be because the ionic liquid diffused out of the gel-state sheet faster in an aqueous ethanol than in air, which meant there was presumably not enough time for hydrogen bonds to rearrange in the latter condition. Consequently, the crystallinity was higher when the films were coagulated in the air.

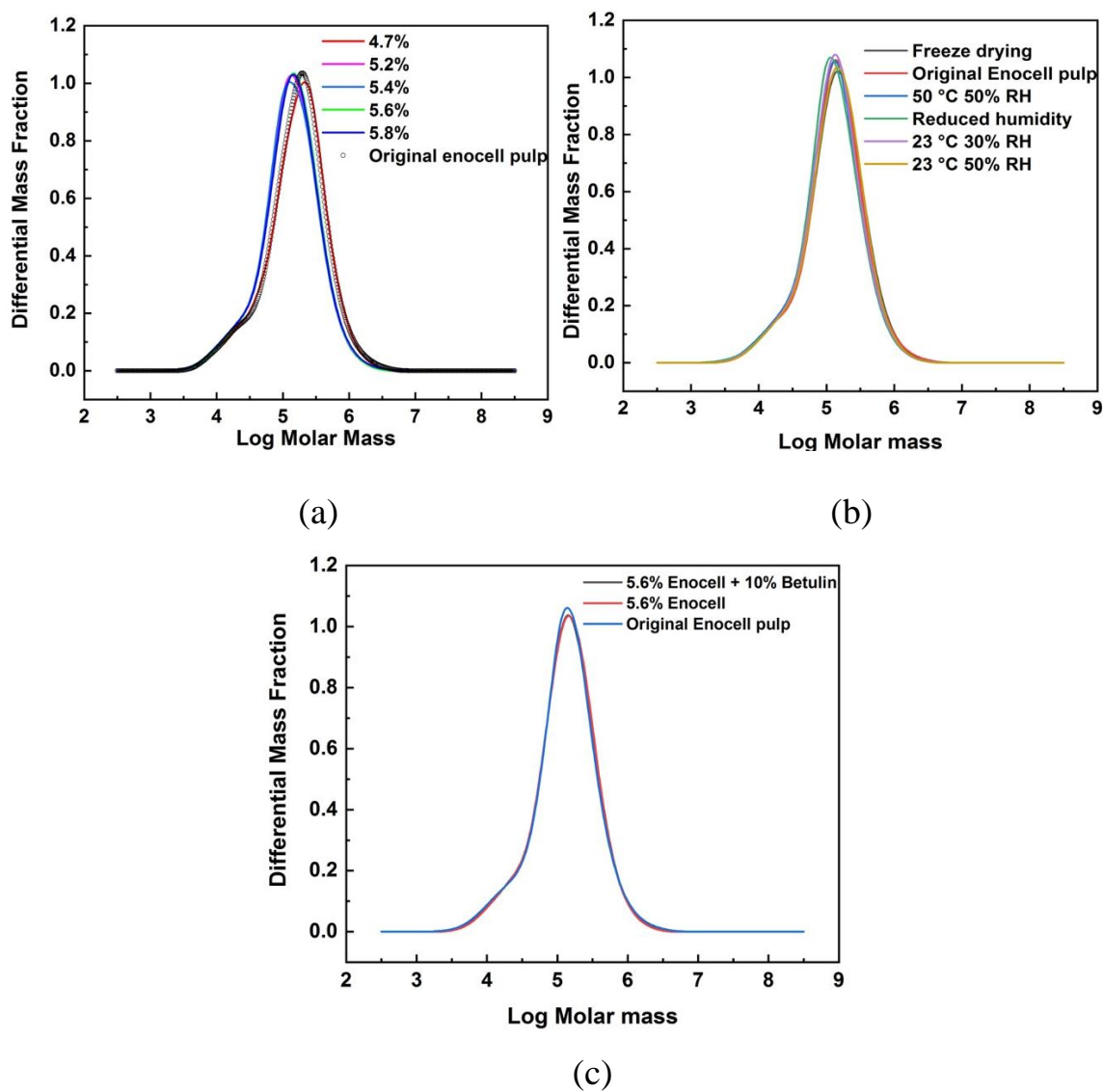


Figure 9. Molecular mass distribution of the original cellulose and the regenerated cellulose films.

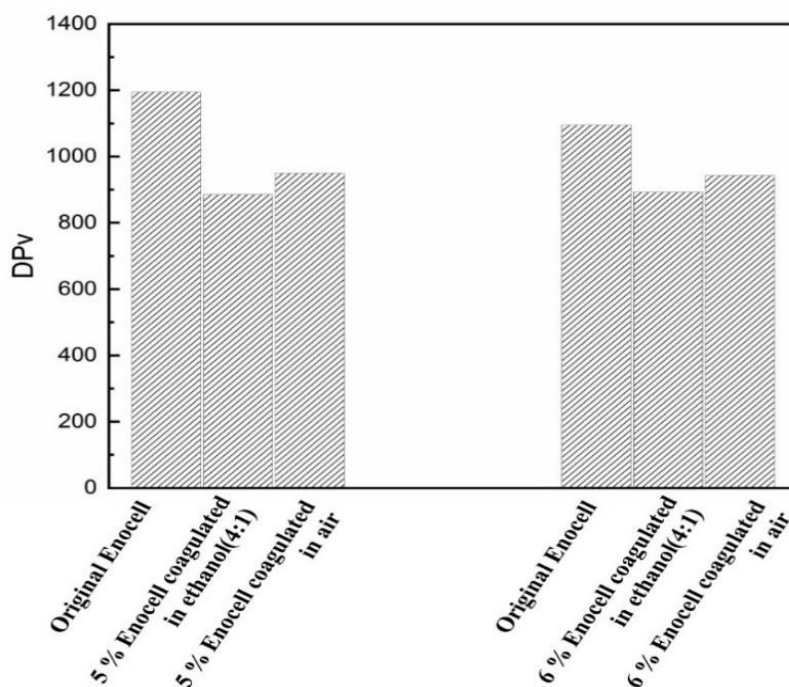


Figure 10. DPv of the original cellulose and the regenerated cellulose films.

4.3.2 Surface morphology and transparency

The drying method and the addition of Betulin affected the appearance of the films extensively, as being presented in Figure 6 (a) and (b). The freeze-dried films showed corrugated surfaces, while the other films dried under a certain humidity showed glossy and shiny surfaces. When the drying temperature increased, the films shrunk rapidly with the presence of a wave shape. The addition of Betulin led to a decrease in transparency of the films.

By observing the top and bottom surfaces of these films via SEM, it could be clearly seen that there was a big difference between the two sides. The surface in contact with the casting substrate was defined as “bottom” and the one in contact with the coagulation bath was referred to “top”. In general, the former was quite smooth, homogeneous and nonporous, whereas the latter presented many tiny pores. This might be caused by the solvent and non-solvent exchange from the top, and non-solvent was penetrated from the first microlayers. [DBNH]OAc molecules in the swollen gel functioned as hydrogen bonders with the

cellulose chains. During the coagulation and regeneration, hydrogen bonds between [DBNH]OAc and the cellulose chains were disrupted, enabling [DBNH]OAc molecules to diffuse out of the network. Simultaneously, new hydrogen bonds between and within the cellulose chains were rebuilt to form a strong network. The positions formerly containing [DBNH]OAc were filled by EtOH and water molecules. After drying, the EtOH and water molecules were volatilized, leaving tiny pores on the surfaces. In contrast, [DBNH]OAc molecules closed to the bottom surface were more likely to be sucked out during the solvent exchange.

Figure 11 displays the SEM images of the regenerated films coagulated in different media, while Figure 12 compares those with and without the addition of Betulin. As explained in chapter 4.1, the coagulated films have a loose structure in the open air, which leads to a lower strength. According to the SEM images of the cross-section, the films were densely packed in the absence of Betulin. On the contrary, both surfaces of the films containing Betulin showed a high roughness due to the aggregates formed from Betulin. The top showed some pores as well. Figure 13 shows cross-sections of the regenerated films made of 5.2 wt%, 5.4wt% and 5.8wt% of cellulose. It did not show many differences between them, except that the films made from 5.4wt% of cellulose had a looser structure.

The drying method had a dramatic influence on the surface morphology of the cast films, based on the images in Figure 14. When drying at the room temperature but different humidity, all the films showed a rough and porous top and a smooth bottom. However, the top was much rougher but less porous when the humidity was reduced step by step from 95 to 55 %, compared to drying in the constant humidity 30 % and 50%. This resulted from the different evaporation rates of ethanol and water at different air humidity. A higher temperature and a lower humidity led to smaller pores, while freeze-drying resulted in a nonporous surface with nubs.

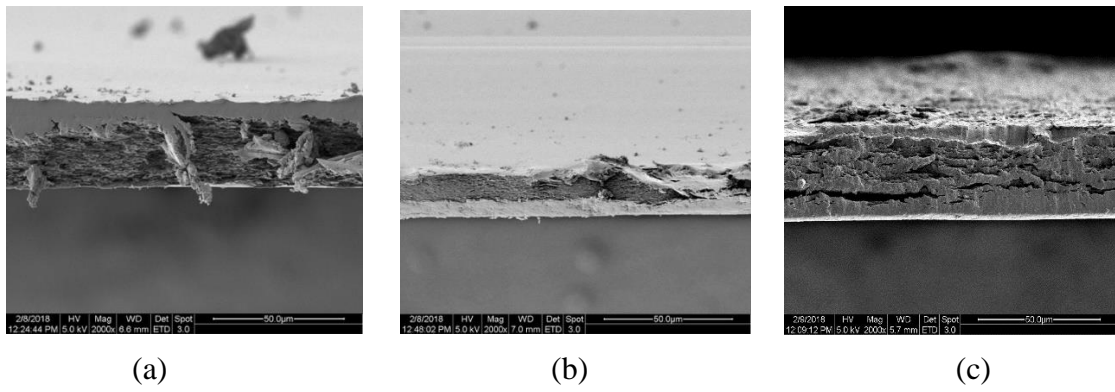


Figure 11. SEM images of the regenerated films coagulated in different baths (a) ethanol:water 1:1 (b) ethanol:water 4:1 (c) open air.

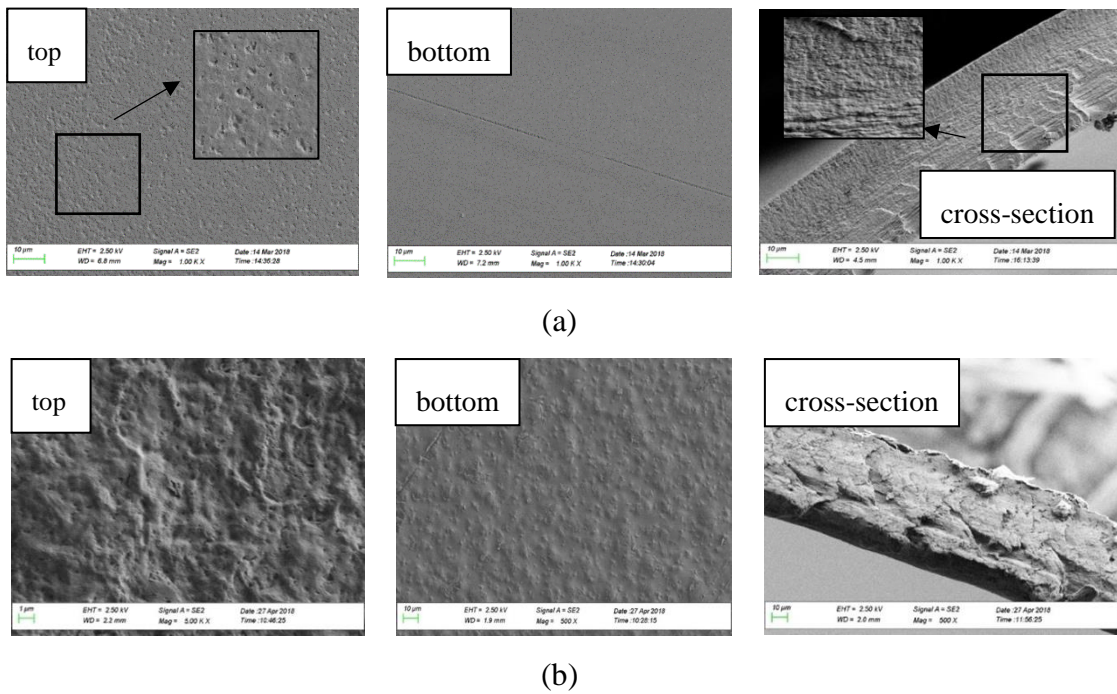


Figure 12. SEM images of the regenerated films (5.6% Enocell) containing (a) with and (b) without 10wt% Betulin.

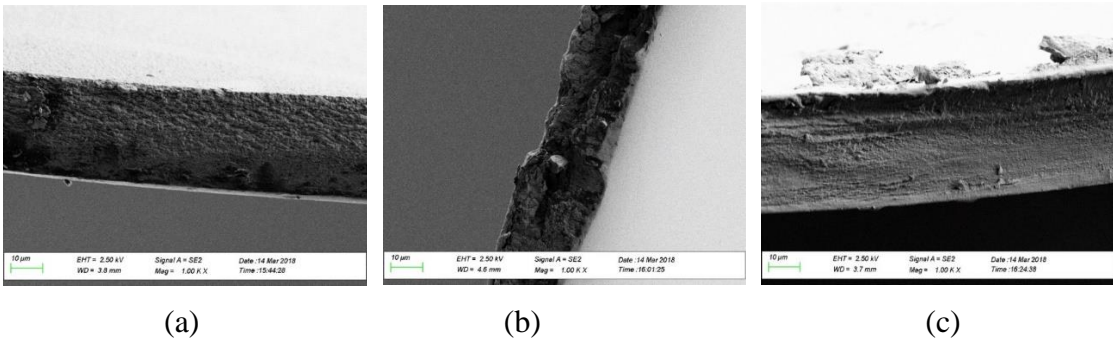
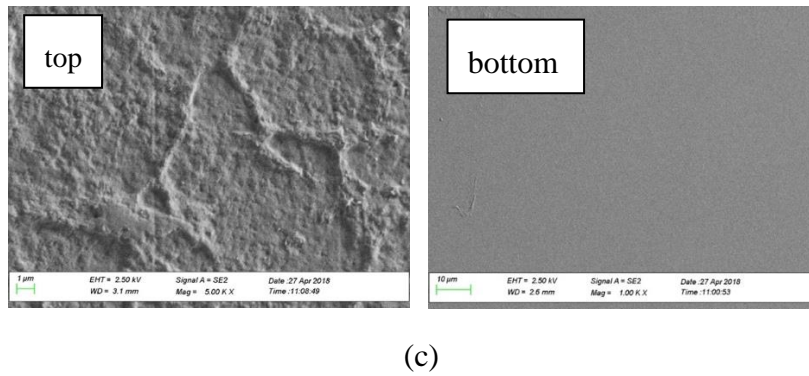
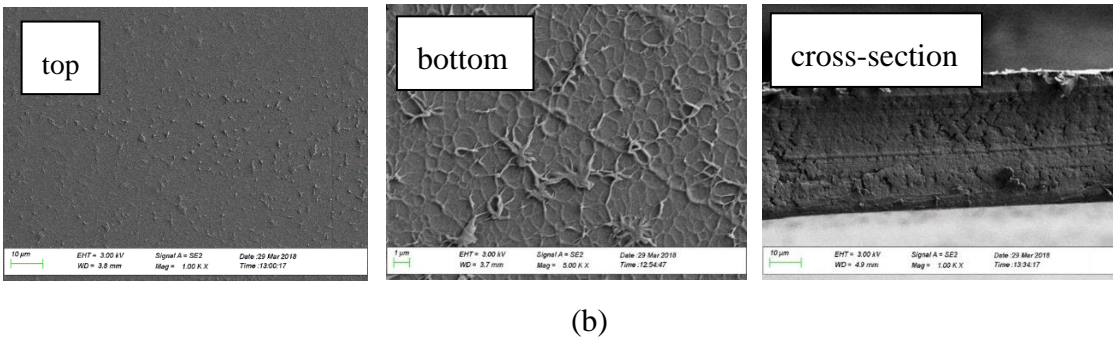
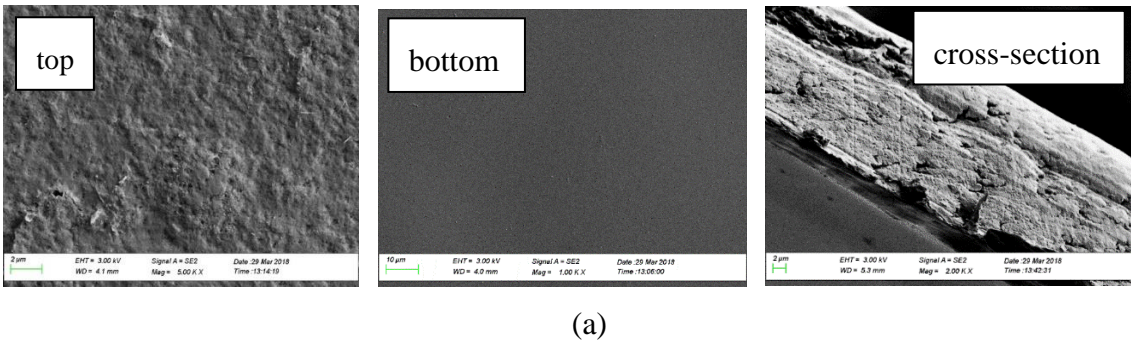
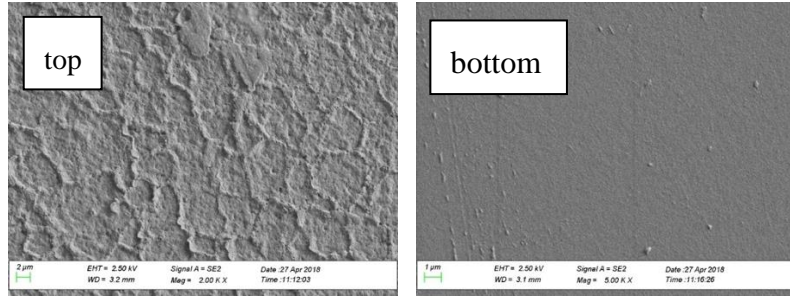


Figure 13. Cross-section images of the regenerated films cast from different concentration of cellulose (a) 5.2 wt% (b) 5.4wt% and (c) 5.8wt%.





(d)

Figure 14. SEM images of the regenerated films (5.6 wt% Enocell) dried under different conditions: (a) Reduced humidity; (b) Freeze drying; (c) 23 °C 30% RH; and (d) 50°C 50% RH.

To accurately characterize the transparency of each film, its transmittance was measured and plotted in Figure 15. All the films were highly transparent with a transmittance above 88%, except for the films containing Betulin due to the aggregations of Betulin. The transparency of the regenerated films from [DBNH][OAc] could be compared to commercial cellophane, which showed an optical transmittance of 92%.

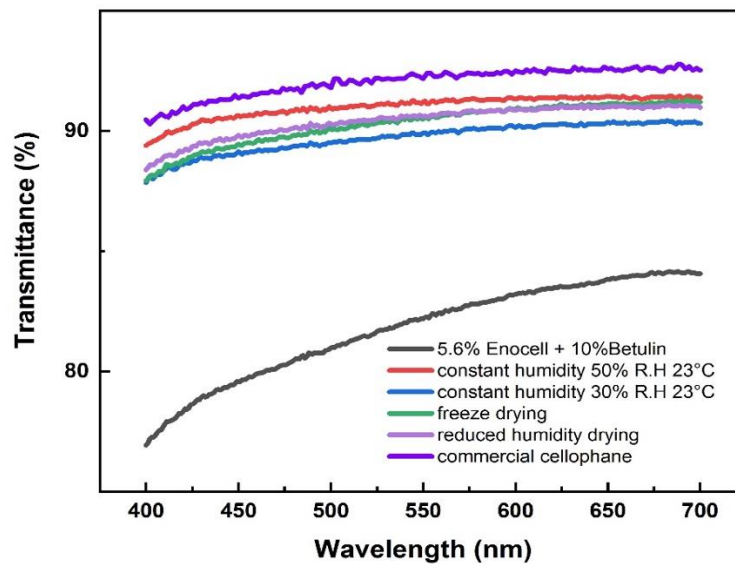


Figure 15. Transmittance of the commercial cellophane and the regenerated cellulose films.

4.3.3 Mechanical properties

The Tensile strength, Young's Modulus and elongation at maximum stress of each film were normalized and recalculated based on the data from the tester, and the commercial cellophane was also measured as a reference. The stress and strain curves of the regenerated films were plotted in Figure 16. Obviously, it could be seen that the commercial cellophane films had a higher tensile strength but a lower elongation than the regenerated cellulose films from [DBNH]OAc. According to the procedure described in this thesis, the regenerated cellulose films were not fully stretched as the commercial cellophane. Thus, the commercial cellophane with an orientation of the fibrils showed higher tenacity.

The concentration of cellulose affected the mechanical properties considerably. Figure 16 (a) also showed a relatively low tensile strength, but a rather high elongation of almost 5% when the cellulose concentration in the dope was 4.7 wt%. In contrast, the films casting from an Enocell solution of 6 wt% resulted in brittle films which easily broke. However, the films regenerated from 5.2 to 5.8 wt% Enocell concentrations performed similarly in terms of the tensile strength and elongation. This proved that there were hardly any differences in the inner structure of these films. As mentioned in chapter 4.3.2, the structure of the films cast from a 5.4 wt% of Enocell solution was loose, which was in accordance with its mechanical performance.

No major differences in the mechanical properties of the regenerated films were found with different drying methods. The tensile strength was around 70 MPa, while the elongation at the max stress was approximately 3%. With the exception of freeze-drying, the films had an exceptionally high elongation of more than 7%. Due to the denser structures of the films containing Betulin, it was only slightly better than the ones without the addition of Betulin, so that the films with a denser structure had a higher tensile strength and lower elongation.

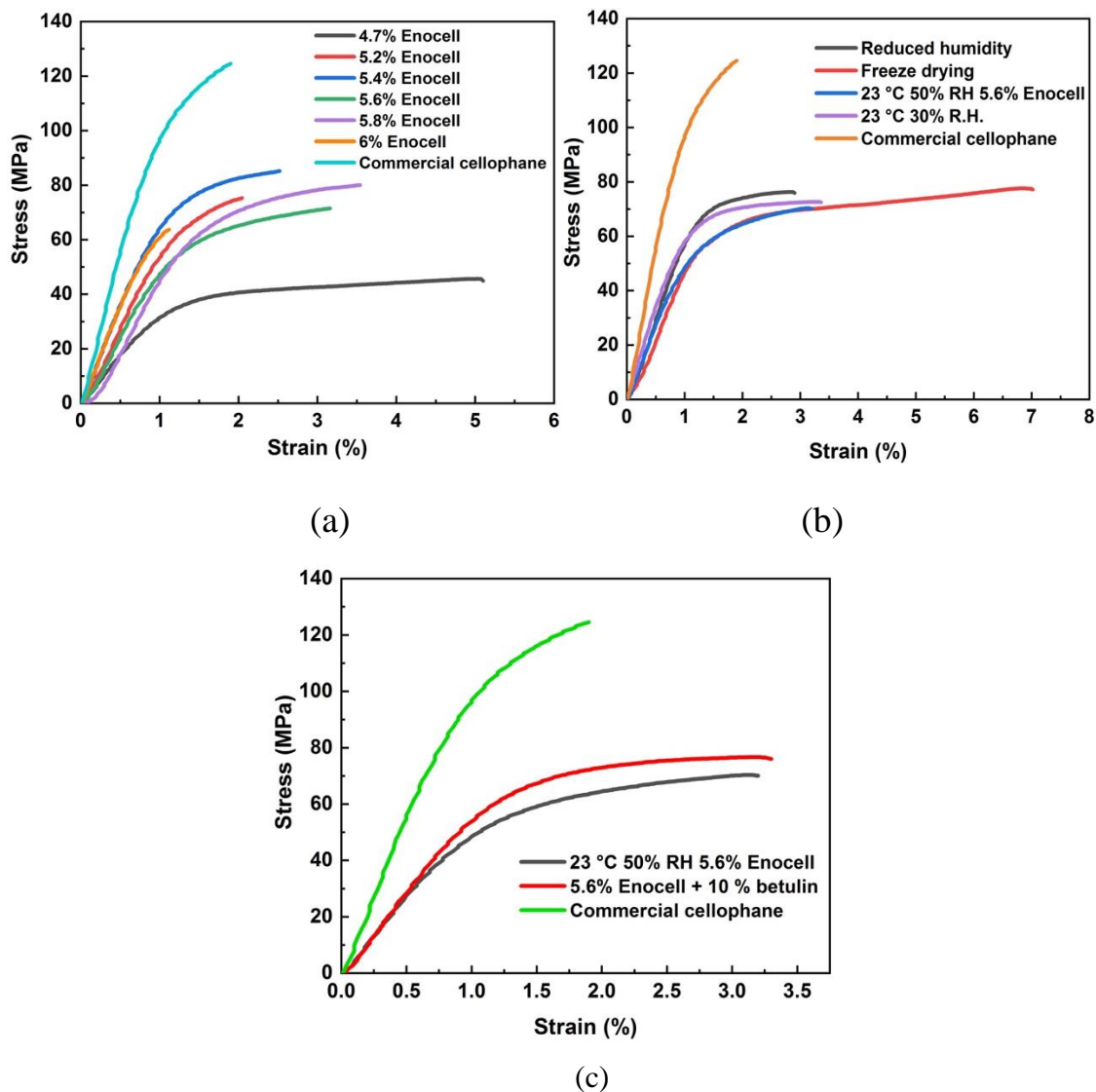


Figure 16. Stress-strain curves of the regenerated cellulose films. (a) with different concentration; (b) with different drying methods; and (c) with or without betulin.

Figure 17 illustrates the relationship between the thickness and the Young's Modulus of each film. The commercial cellophane was thinner with excellent properties. The thickness of the regenerated cellulose films from [DBNH]OAc was determined between 27 and 31 μm . The Young's Modulus of the films with different percentages of Enocell was between 6 GPa and 8 GPa, except for the films of 4.7 wt%, which performed the lowest due to an insufficient cellulose network. In addition, the films with Betuin were thicker, but showed a similar level of the Young's Modulus. The films dried at 23 °C and 30% RH were stronger to resist deformation (Young's Modulus of 7.5 GPa) than those dried at a higher and at a

reduced humidity (Young's Modulus of 6.2 and 7.2 GPa respectively). Freeze drying resulted in a lower Young's Modulus.

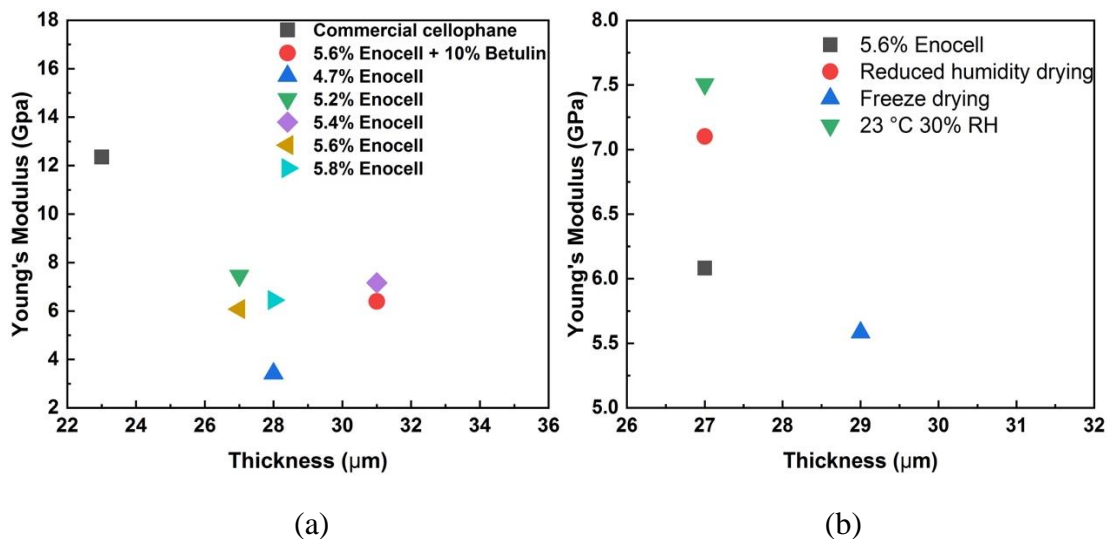


Figure 17. The relationship between thickness and Young's Modulus of regenerated cellulose films (a) with different concentration; (b) containing 5.6 wt% Enocell pulp but with different drying methods.

4.3.4 Thermal stability

The TG curves of original Enocell pulp and the regenerated cellulose films are shown in Figure 18. A small weight loss was shown in all the samples, except for the original Enocell pulp, which maintained its weight unbelow 250°C . This loss should correspond to the loss of the bound and absorbed water. The original cellulose had a slightly higher decomposition temperature, thus a higher thermal stability. Since after regeneration, the crystallinity of cellulose usually decreases, it was much easier to decompose cellulose chains. Figure 18(b) shows that the thermal stability of the regenerated films was barely influenced by the drying conditions. The decomposition temperature was increased and the thermal stability improved when the films consisted of cellulose and Betulin.

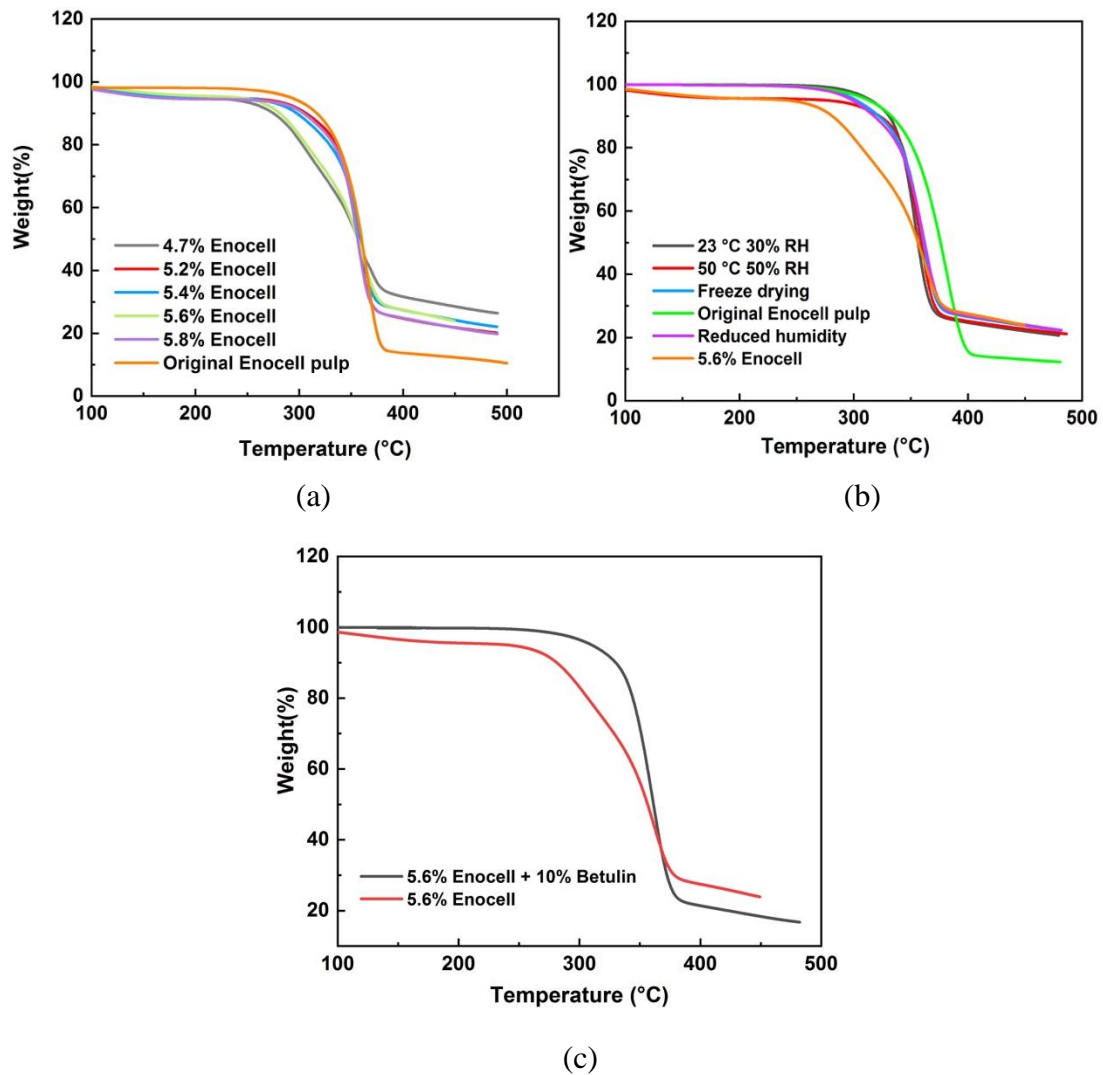


Figure 18. The TG curves of original cellulose and regenerated cellulose films. (a) with different concentrations; (b) dried with different methods and (c) with addition of betulin.

4.3.5 Water vapor permeability

As Figure 19 shows, according to the relationship between the weight changes of cups and the time, a slope could be obtained, based on which WVTR and WVP were calculated sequentially. The results are listed in Table 2. The film with Betulin was more homogeneous in terms of water vapor permeability, since two samples gave almost the same value ($3300 \text{ g} \cdot \mu\text{m}/\text{m}^2 \cdot \text{day} \cdot \text{kPa}$). It indicated that Betulin aggregates are evenly dispersed, thus enhancing the homogeneity. However, all films presented poor barrier water vapor property with a WVTR of $3300\text{-}4020 \text{ g} \cdot \mu\text{m}/\text{m}^2 \cdot \text{day} \cdot \text{kPa}$. This large range of high water vapor permeability can be attributed to the tiny holes on the surface. They form channels through

which water molecules can pass. These films can be applied as bakery product packaging mainly.

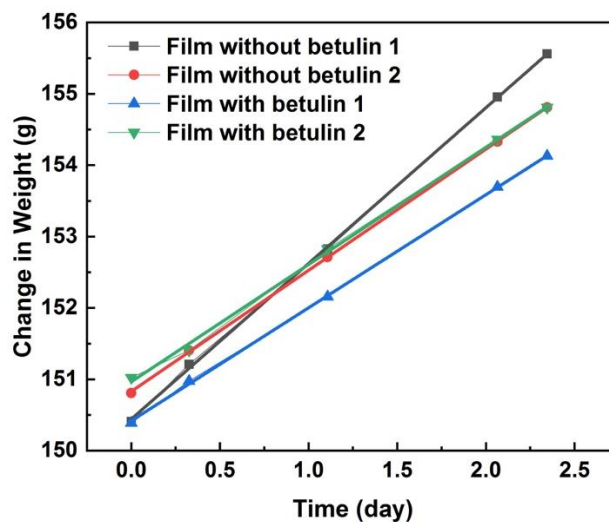


Figure 19. The relationship between the weight gains of cups containing the films and the time.

Table 2. Results of calculating WVTR and WVP.

Sample	Saturated pressure 1.237 %R.H.				
	No	Average thickness (μm)	Slope (g/day)	WVTR ($g/m^2 \cdot day$)	WVP ($g \cdot \mu m/m^2 \cdot day \cdot kPa$)
No Betulin in the films	1	31.2	2.18	159.40	4019.55
	2	32.6	1.70	124.05	3368.85
Containing Betulin	1	35.6	2.58	115.77	3330.94
	2	34.6	2.64	120.06	3357.46

4.3.6 Hydrophilicity

The contact angles were measured on three spots of each regenerated cellulose film containing without and with Betulin. The photos of the water droplets onto the films were displayed in Figure 20 and the values were listed in Table 3. It was clearly observed that the

film without Betulin inside were very hydrophilic (contact angle of 27.5° in average), but the one with Betulin presented a lower hydrophilicity (contact angle of 71.5° in average). Furthermore, the contact angles in three spots of the films without Betulin were almost invariable, only with a deviation of 1.7° . This indicated that the films fabricated with the solution containing Betulin had a less homogeneous surface. Based on the SEM images discussed in chapter 4.3.2, the Betulin aggregates were homodispersed on the surface, which led to an improvement of its hydrophobicity. From this it could be inferred that the blending method was effective to modify the regenerated film surface and to change the wettability.

Table 3. Contact angle of each film.

	Films without Betulin			Films with Betulin		
	Spot 1	Spot 2	Spot 3	Spot 1	Spot 2	Spot 3
Contact Angle/ $^{\circ}$	25.5 ± 0.4	29.3 ± 0.9	26.3 ± 1.1	73.4 ± 4.2	70.7 ± 2.3	67.7 ± 4.1
Deviation/ $^{\circ}$	1.7			2.3		

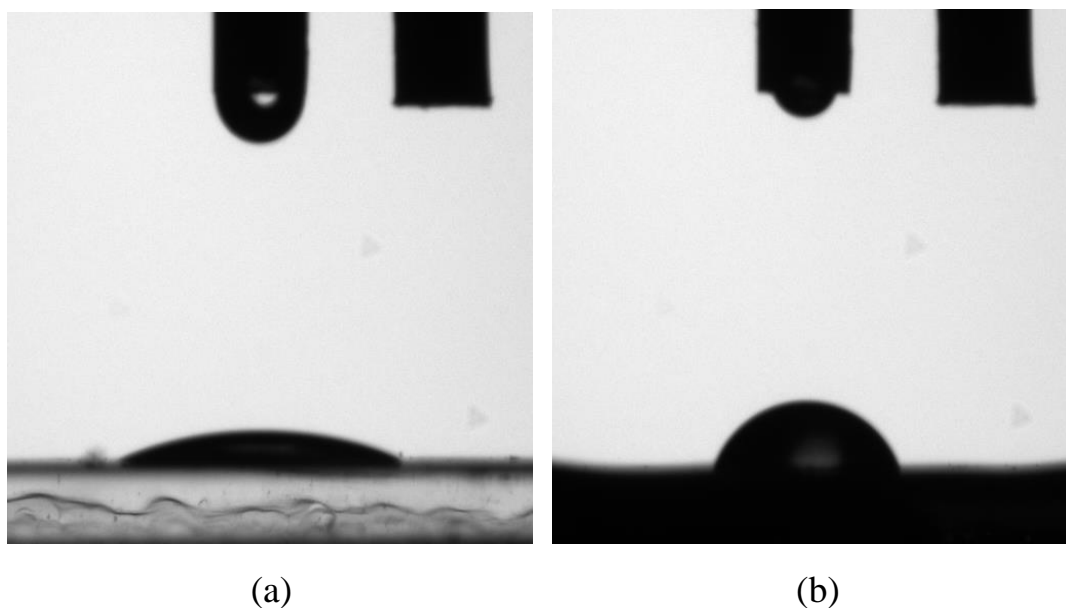


Figure 20. Contact angle of regenerated cellulose films (a) without and (b) with addition of

Betulin.

4.3.7 Efficiency of removing IL ([DBNH]OAc) by deionized water

Table 4. Elemental analysis of nitrogen, oxygen, carbon and hydrogen in regenerated films and original Enocell pulp.

Type of film	Mol Ratio			
	C/C	H/C	O/C	N/C
RCF-4.7	1	1.856	0.850	0.0034
RCF-5.2	1	1.645	0.882	0.0023
RCF-5.4	1	1.242	0.946	0.0037
RCF-5.6	1	2.000	0.876	0.0080
RCF-5.8	1	1.898	0.882	0.0025
Enocell	1	1.861	0.852	0.0040

The element contents of nitrogen, oxygen, carbon and hydrogen in the regenerated films and the original Enocell pulp were listed in Table 4. It could be seen that the ratio of nitrogen-to-carbon of each film was in the range 2 to 4×10^{-3} magnitude which implies that washing of the regenerated films in deionized water by immersion was efficient to remove the residual ionic liquid.

5. Conclusion

Highly transparent films could be regenerated from [DBNH][OAc]/Enocell solutions. As expected, the complex viscosity and moduli of cellulose/[DBNH]OAc solutions were concentration-dependent. The insoluble aggregates of Betulin increased the complex viscosity considerably.

The final properties of the films were determined by various parameters during casting, coagulation or regeneration and drying. The cellulose concentration influenced primarily the mechanical properties of the films. The optimum Enocell concentration of casting films from the [DBNH][OAc] solution has been proven to be between 5 wt% to 6 wt%, as the films cast from the solution of 5 wt% were transparent, strong and flexible, while the films were brittle and opaque from the solution with the concentration of 6wt%. The films prepared from a 4 wt% Enocell solution showed an extraordinary shrinkage. Subsequent experiments revealed that 5.6 wt% and 5.8 wt% were the optimum Enocell concentrations. The films from these Enocell concentrations had a tensile strength of 70-80 MPa, an elongation of 3-3.5% and a Young's Modulus of 5 GPa. These regenerated cellulose films were just stretched slightly with the tape, so the tensile strength of the regenerated films was lower than that of the commercial cellophane. It could be concluded that the mechanical properties would be considerably improved due to the orientation of the cellulose molecules and microfibrils. Nonetheless, the mechanical properties were not very dependent on the drying methods. The drying process only affected the surface morphology, since the EtOH and deionized water in wet films were evaporated with different rates when applying the different drying methods, leaving pores with different size on the top surfaces.

The MMD results did not differ much from the original cellulose materials and the regenerated cellulose films or from different drying methods. This indicated that only limited polymer degradation occurs during both during the dissolution and regeneration processes

and during drying. The decomposition temperature of fresh pulp is slightly higher, which shows a higher thermal stability of Enocell pulp than that of the regenerated cellulose. This could result from the reduction of crystallinity and the conversion of the crystal structure to cellulose II.

When blending a hydrophobic agent (Betulin) with Enocell pulp during dissolution, Betulin particles aggregated together. With the presence of 10 % Betulin, the films displayed a higher contact angle, but they still remained hydrophilic. Unfortunately, the addition of Betulin to the cellulose has not improved the water vapor barrier properties as shown by the very high water vapor permeability ($3000-4000 \text{ g} \cdot \mu\text{m}/\text{m}^2 \cdot \text{day} \cdot \text{kPa}$).

For the future work, since it was not possible to compare the crystallinity of the original and the regenerated cellulose and the oxygen permeability of them due to the breakage of the equipment, it would be vital to analyze the cellulose structure transformation during regeneration. In addition, the oxygen permeability should be examined in the future when used in packaging.

It is worth stretching the films in different directions to obtain oriented, stronger and more homogenous samples. Since the [DBNH][OAc]/Enocell solution system has been proven to be excellent to dry-jet wet spinning textile fibers, it is definitely worth refining the collection rollers especially for film spinning in comparison to the paths described in Appendix 2.

Reference

- Berggren, Rickard, Fredrik Berthold, Elisabeth Sjöholm, and Mikael Lindström. 2003. "Improved Methods for Evaluating the Molar Mass Distributions of Cellulose in Kraft Pulp." *Journal of Applied Polymer Science* 88 (5): 1170–79. <https://doi.org/10.1002/app.11767>.
- Cai, Tao, Huihui Zhang, Qinghua Guo, Huili Shao, and Xuechao Hu. 2010. "Structure and Properties of Cellulose Fibers from Ionic Liquids." *Journal of Applied Polymer Science* 115 (2). Wiley-Blackwell: 1047–53. <https://doi.org/10.1002/app.31081>.
- Chang, Chunyu, and Lina Zhang. 2011. "Cellulose-Based Hydrogels: Present Status and Application Prospects." *Carbohydrate Polymers* 84 (1): 40–53. <https://doi.org/10.1016/j.carbpol.2010.12.023>.
- Chen, Xun, Yumei Zhang, Huaping Wang, Shih-Wa Wang, Siwei Liang, and Ralph H. Colby. 2011. "Solution Rheology of Cellulose in 1-Butyl-3-Methyl Imidazolium Chloride." *Journal of Rheology* 55 (3): 485–94. <https://doi.org/10.1122/1.3553032>.
- Dawsey, T. R., and C. L. McCormick. 1990. "THE LITHIUM CHLORIDE/DIMETHYLACETAMIDE SOLVENT FOR CELLULOSE: A LITERATURE REVIEW." *Journal of Macromolecular Science, Part C* 30 (3–4). Taylor & Francis Group : 405–40. <https://doi.org/10.1080/07366579008050914>.
- Feng, Li, and Zhong-lan Chen. 2008. "Research Progress on Dissolution and Functional Modification of Cellulose in Ionic Liquids." *Journal of Molecular Liquids* 142 (1–3). Elsevier: 1–5. <https://doi.org/10.1016/J.MOLLIQ.2008.06.007>.
- Fink, H. P., P. Weigel, H. J. Purz, and J. Ganster. 2001. "Structure Formation of Regenerated Cellulose Materials from NMMO-Solutions." *Progress in Polymer Science (Oxford)* 26 (9): 1473–1524. [https://doi.org/10.1016/S0079-6700\(01\)00025-9](https://doi.org/10.1016/S0079-6700(01)00025-9).
- Fink, Hans-Peter, Johannes Ganster, and André Lehmann. 2014. "Progress in Cellulose Shaping: 20 Years Industrial Case Studies at Fraunhofer IAP." *Cellulose* 21 (1).

Springer Netherlands: 31–51. <https://doi.org/10.1007/s10570-013-0137-7>.

Fink, Hans-Peter, Peter Weigel, and Andreas Bohn. 1999. “Supermolecular Structure and Orientation of Blown Cellulosic Films.” *Journal of Macromolecular Science, Part B* 38 (5–6). Taylor & Francis Group : 603–13.

<https://doi.org/10.1080/00222349908248124>.

Fort, DA, RC Remsing, RP Swatloski, ... P Moyna - Green, and undefined 2007. n.d. “Can Ionic Liquids Dissolve Wood? Processing and Analysis of Lignocellulosic Materials with 1-n-Butyl-3-Methylimidazolium Chloride.” *Pubs.Rsc.Org*. Accessed April 24, 2018. <http://pubs.rsc.org/en/content/articlehtml/2007/gc/b607614a>.

French, Alfred D. 2017. “Glucose, Not Cellobiose, Is the Repeating Unit of Cellulose and Why That Is Important.” *Cellulose* 24 (11): 4605–9. <https://doi.org/10.1007/s10570-017-1450-3>.

Fukaya, Yukinobu, Kensaku Hayashi, Masahisa Wada, and Hiroyuki Ohno. 2008.

“Cellulose Dissolution with Polar Ionic Liquids under Mild Conditions: Required Factors for Anions.” *Green Chem.* 10 (1). Royal Society of Chemistry: 44–46.

<https://doi.org/10.1039/B713289A>.

Gan, Sinyee, Sarani Zakaria, Chin Hua Chia, Ruey Shan Chen, Amanda V. Ellis, and Hatika Kaco. 2017. “Highly Porous Regenerated Cellulose Hydrogel and Aerogel Prepared from Hydrothermal Synthesized Cellulose Carbamate.” Edited by Yogendra Kumar Mishra. *PLOS ONE* 12 (3). Public Library of Science: e0173743.

<https://doi.org/10.1371/journal.pone.0173743>.

Guidotti, Tee L. 2017. “Blanc PD Fake Silk: The Lethal History of Viscose Rayon. New Haven, CT: Yale University Press, 2016. 309 Pp. ISBN 978-0-300-20466-7.” *Risk Analysis* 37 (4). Wiley/Blackwell (10.1111): 840–42.

<https://doi.org/10.1111/risa.12808>.

Hao Zhang, Jin Wu, * and Jun Zhang, and Jiasong He. 2005. “1-Allyl-3-Methylimidazolium Chloride Room Temperature Ionic Liquid: A New and Powerful Nonderivatizing Solvent for Cellulose.” American Chemical Society .

<https://doi.org/10.1021/MA0505676>.

Hauru, Lauri K. J., Michael Hummel, Anne Michud, and Herbert Sixta. 2014. "Dry Jet-Wet Spinning of Strong Cellulose Filaments from Ionic Liquid Solution." *Cellulose* 21 (6). Springer Netherlands: 4471–81. <https://doi.org/10.1007/s10570-014-0414-0>.

Hauru, LKJ, M Hummel, A Michud, H Sixta - Cellulose, and undefined 2014. n.d. "Dry Jet-Wet Spinning of Strong Cellulose Filaments from Ionic Liquid Solution." *Springer*. Accessed April 25, 2018.

https://idp.springer.com/authorize/casa?redirect_uri=https://link.springer.com/article/10.1007/s10570-014-0414-0&casa_token=YONvzvahYKwAAAAA:nDfOWhXma-dqi1ajTJdKmjUDXIjb0CG_FEOJglr_OJpauMCkxcao0PsIVbjObjUCCWloHJBYDt3bCPj9.

Heinze, Thomas, Katrin Schwikal, and Susann Barthel. 2005. "Ionic Liquids as Reaction Medium in Cellulose Functionalization." *Macromolecular Bioscience* 5 (6). Wiley-Blackwell: 520–25. <https://doi.org/10.1002/mabi.200500039>.

Huang, Tianxiao, Dongfang Li, and Monica Ek. 2018. "Water Repellency Improvement of Cellulosic Textile Fibers by Betulin and a Betulin-Based Copolymer." *Cellulose* 25 (3). Springer Netherlands: 2115–28. <https://doi.org/10.1007/s10570-018-1695-5>.

Hummel, Michael, Anne Michud, Marjaana Tanttu, Shirin Asaadi, Yibo Ma, Lauri K. J. Hauru, Arno Parviainen, Alistair W. T. King, Ilkka Kilpeläinen, and Herbert Sixta. 2015. "Ionic Liquids for the Production of Man-Made Cellulosic Fibers: Opportunities and Challenges." In . https://doi.org/10.1007/12_2015_307.

Kilpeläinen, Ilkka, Haibo Xie, Alistair King, Mari Granstrom, Sami Heikkinen, and Dimitris S. Argyropoulos. 2007. "Dissolution of Wood in Ionic Liquids." *Journal of Agricultural and Food Chemistry* 55 (22): 9142–48. <https://doi.org/10.1021/jf071692e>.

Kimura, Mutsumi, Yoshie Shinohara, Junko Takizawa, Sixiao Ren, Kento Sagisaka, Yudeng Lin, Yoshiyuki Hattori, and Juan P. Hinestroza. 2015. "Versatile Molding Process for Tough Cellulose Hydrogel Materials." *Scientific Reports* 5 (1). Nature

Publishing Group: 16266. <https://doi.org/10.1038/srep16266>.

Klemm, Dieter, Brigitte Heublein, Hans-Peter Fink, and Andreas Bohn. 2005. "Cellulose: Fascinating Biopolymer and Sustainable Raw Material." *Angewandte Chemie International Edition* 44 (22). Wiley-Blackwell: 3358–93.

<https://doi.org/10.1002/anie.200460587>.

Laus, Gerhard, Gino Bentivoglio, Herwig Schottenberger, Volker Kahlenberg, Holger Kopacka, Thomas Röder, and Herbert Sixta. 2005. "IONIC LIQUIDS: CURRENT DEVELOPMENTS, POTENTIAL AND DRAWBACKS FOR INDUSTRIAL APPLICATIONS." *Lenzinger Berichte* 84: 71–85.

https://www.researchgate.net/profile/Herwig_Schottenberger/publication/228666834_Ionic_liquids_Current_developments_potential_and_drawbacks_for_industrial_applications/links/02e7e52663544d1611000000.pdf.

Li, R, L Zhang, M Xu - Carbohydrate polymers, and undefined 2012. n.d. "Novel Regenerated Cellulose Films Prepared by Coagulating with Water: Structure and Properties." *Elsevier*. Accessed May 1, 2018.

<https://www.sciencedirect.com/science/article/pii/S0144861711005996>.

Liang, Songmiao, Lina Zhang, Yanfang Li, and Jian Xu. 2007. "Fabrication and Properties of Cellulose Hydrated Membrane with Unique Structure." *Macromolecular Chemistry and Physics* 208 (6): 594–602. <https://doi.org/10.1002/macp.200600579>.

Lina Zhang, *, and Dong Ruan, and Jinping Zhou. 2001. "Structure and Properties of Regenerated Cellulose Films Prepared from Cotton Linters in NaOH/Urea Aqueous Solution." *American Chemical Society* . <https://doi.org/10.1021/IE0010417>.

Lina Zhang, *, Yuan Mao, and Jinping Zhou, and Jie Cai. 2005. "Effects of Coagulation Conditions on the Properties of Regenerated Cellulose Films Prepared in NaOH/Urea Aqueous Solution." *American Chemical Society* . <https://doi.org/10.1021/IE0491802>.

Liu, Shilin, and Lina Zhang. 2009. "Effects of Polymer Concentration and Coagulation Temperature on the Properties of Regenerated Cellulose Films Prepared from

- LiOH/Urea Solution.” *Cellulose* 16 (2). Springer Netherlands: 189–98.
<https://doi.org/10.1007/s10570-008-9268-7>.
- Liu, Zhen, Hui Wang, Zengxi Li, Xingmei Lu, Xiangping Zhang, Suojiang Zhang, and Kebin Zhou. 2011. “Characterization of the Regenerated Cellulose Films in Ionic Liquids and Rheological Properties of the Solutions.” *Materials Chemistry and Physics* 128 (1–2). Elsevier: 220–27.
<https://doi.org/10.1016/J.MATCHEMPHYS.2011.02.062>.
- Ma, Yibo, Jonas Stubb, Inkeri Kontro, Kaarlo Nieminen, Michael Hummel, and Herbert Sixta. 2018. “Filament Spinning of Unbleached Birch Kraft Pulps: Effect of Pulping Intensity on the Processability and the Fiber Properties.” *Carbohydrate Polymers* 179 (January): 145–51. <https://doi.org/10.1016/j.carbpol.2017.09.079>.
- Mazza, Mathieu, Dan-Andrei Catana, Carlos Vaca-Garcia, and Christine Cecutti. 2009. “Influence of Water on the Dissolution of Cellulose in Selected Ionic Liquids.” *Cellulose* 16 (2). Springer Netherlands: 207–15. <https://doi.org/10.1007/s10570-008-9257-x>.
- McCormick, Charles L., and Peter A. Callais. 1987. “Derivatization of Cellulose in Lithium Chloride and N-N-Dimethylacetamide Solutions.” *Polymer* 28 (13). Elsevier: 2317–23. [https://doi.org/10.1016/0032-3861\(87\)90393-4](https://doi.org/10.1016/0032-3861(87)90393-4).
- Medronho, B, B Lindman - Current Opinion in Colloid & Interface Science, and undefined. 2014. n.d. “Competing Forces during Cellulose Dissolution: From Solvents to Mechanisms.” *Elsevier*. Accessed May 12, 2018.
<https://www.sciencedirect.com/science/article/pii/S1359029413001350>.
- Michud, Anne, Michael Hummel, and Herbert Sixta. 2015. “Influence of Molar Mass Distribution on the Final Properties of Fibers Regenerated from Cellulose Dissolved in Ionic Liquid by Dry-Jet Wet Spinning.” *Polymer* 75 (September): 1–9.
<https://doi.org/10.1016/j.polymer.2015.08.017>.
- Michud, Anne, Marjaana Tanttu, Shirin Asaadi, Yibo Ma, Eveliina Netti, Pirjo Kääriäinen, Anders Persson, Anders Berntsson, Michael Hummel, and Herbert Sixta. 2016.

- “Ioncell-F: Ionic Liquid-Based Cellulosic Textile Fibers as an Alternative to Viscose and Lyocell.” *Textile Research Journal* 86 (5). SAGE PublicationsSage UK: London, England: 543–52. <https://doi.org/10.1177/0040517515591774>.
- Moon, Robert J., Ashlie Martini, John Nairn, John Simonsen, and Jeff Youngblood. 2011. “Cellulose Nanomaterials Review: Structure, Properties and Nanocomposites.” *Chemical Society Reviews* 40 (7). The Royal Society of Chemistry: 3941. <https://doi.org/10.1039/c0cs00108b>.
- Pang, JinHui, Miao Wu, QiaoHui Zhang, Xin Tan, Feng Xu, XueMing Zhang, and RunCang Sun. 2015. “Comparison of Physical Properties of Regenerated Cellulose Films Fabricated with Different Cellulose Feedstocks in Ionic Liquid.” *Carbohydrate Polymers* 121 (May). Elsevier: 71–78. <https://doi.org/10.1016/J.CARBPOL.2014.11.067>.
- Parviainen, A, AWT King, ... I Mutikainen -, and undefined 2013. n.d. “Predicting Cellulose Solvating Capabilities of Acid–Base Conjugate Ionic Liquids.” *Wiley Online Library*. Accessed May 2, 2018. <http://onlinelibrary.wiley.com/doi/10.1002/cssc.201300143/full>.
- Pinkert, André, Kenneth N. Marsh, Shusheng Pang, and Mark P. Staiger. 2009a. “Ionic Liquids and Their Interaction with Cellulose.” *Chemical Reviews* 109 (12). American Chemical Society: 6712–28. <https://doi.org/10.1021/cr9001947>.
- . 2009b. “Ionic Liquids and Their Interaction with Cellulose.” *Chemical Reviews* 109 (12). American Chemical Society: 6712–28. <https://doi.org/10.1021/cr9001947>.
- . 2009c. “Ionic Liquids and Their Interaction with Cellulose.” *Chemical Reviews* 109 (12): 6712–28. <https://doi.org/10.1021/cr9001947>.
- “Process for the Preparation of Cellulose Sheet.” 1994, March. [https://patents.google.com/patent/US6258304B1/en?assignee=Lenzing+AG&before=priority:19971231&after=priority:19970101&oq=assignee:\(Lenzing+AG\)+1997+](https://patents.google.com/patent/US6258304B1/en?assignee=Lenzing+AG&before=priority:19971231&after=priority:19970101&oq=assignee:(Lenzing+AG)+1997+).
- Pu, Yunqiao, Nan Jiang, and Arthur J. Ragauskas. 2007. “Ionic Liquid as a Green Solvent for Lignin.” *Journal of Wood Chemistry and Technology* 27 (1). Taylor & Francis

Group : 23–33. <https://doi.org/10.1080/02773810701282330>.

- Qi, Haisong, Chunyu Chang, and Lina Zhang. 2009. “Properties and Applications of Biodegradable Transparent and Photoluminescent Cellulose Films Prepared via a Green Process.” *Green Chem.* 11 (2): 177–84. <https://doi.org/10.1039/B814721C>.
- Reddy, Narendra, and Yiqi Yang. 2015. “The N-Methylmorpholine-N-Oxide (NMMO) Process of Producing Regenerated Fibers.” In *Innovative Biofibers from Renewable Resources*, 65–71. Berlin, Heidelberg: Springer Berlin Heidelberg. https://doi.org/10.1007/978-3-662-45136-6_18.
- Remsing, Richard C., Richard P. Swatloski, Robin D. Rogers, and Guillermo Moyna. 2006. “Mechanism of Cellulose Dissolution in the Ionic Liquid 1-n-Butyl-3-Methylimidazolium Chloride: A ¹³C and ^{35/37}Cl NMR Relaxation Study on Model Systems.” *Chemical Communications* 0 (12). The Royal Society of Chemistry: 1271. <https://doi.org/10.1039/b600586c>.
- Rodrigues Filho, Guimes, and Rosana Maria Nascimento de Assunção. 1993. “Application of the Cuprammonium Process (Process for the Production of Regenerated Cellulose Membranes for Hemodialysis) to Sugar-Cane Bagasse.” *Journal of Membrane Science* 82 (1–2). Elsevier: 43–49. [https://doi.org/10.1016/0376-7388\(93\)85091-A](https://doi.org/10.1016/0376-7388(93)85091-A).
- Rosenau, Thomas, Antje Potthast, Herbert Sixta, and Paul Kosma. 2001. “The Chemistry of Side Reactions and Byproduct Formation in the System NMMO/Cellulose (Lyocell Process).” *Progress in Polymer Science* 26 (9). Pergamon: 1763–1837. [https://doi.org/10.1016/S0079-6700\(01\)00023-5](https://doi.org/10.1016/S0079-6700(01)00023-5).
- Saha, Satyen, Satoshi Hayashi, Akiko Kobayashi, and Hiro-o Hamaguchi. 2003. “Crystal Structure of 1-Butyl-3-Methylimidazolium Chloride. A Clue to the Elucidation of the Ionic Liquid Structure.” *Chemistry Letters* 32 (8). The Chemical Society of Japan 公益社団法人 日本化学会 : 740–41. <https://doi.org/10.1246/cl.2003.740>.
- Sammons, R. J., J. R. Collier, T. G. Rials, and S. Petrovan. 2008. “Rheology of 1-Butyl-3-Methylimidazolium Chloride Cellulose Solutions. I. Shear Rheology.” *Journal of*

Applied Polymer Science 110 (2). Wiley-Blackwell: 1175–81.

<https://doi.org/10.1002/app.28733>.

Schulz, L, B Seger, W Burchard - chemistry and physics, and undefined 2000. n.d.

“Structures of Cellulose in Solution.” *Wiley Online Library*. Accessed April 25, 2018.

[https://onlinelibrary.wiley.com/doi/abs/10.1002/1521-](https://onlinelibrary.wiley.com/doi/abs/10.1002/1521-3935(20001001)201:15%3C2008::AID-MACP2008%3E3.0.CO;2-H)

[3935\(20001001\)201:15%3C2008::AID-MACP2008%3E3.0.CO;2-H](https://onlinelibrary.wiley.com/doi/abs/10.1002/1521-3935(20001001)201:15%3C2008::AID-MACP2008%3E3.0.CO;2-H).

Schulz, Liane, Bernd Seger, and Walther Burchard. 2000. “Structures of Cellulose in Solution.” *Macromolecular Chemistry and Physics* 201 (15): 2008–22.

[https://doi.org/10.1002/1521-3935\(20001001\)201:15<2008::AID-](https://doi.org/10.1002/1521-3935(20001001)201:15<2008::AID-MACP2008>3.0.CO;2-H)

[MACP2008>3.0.CO;2-H](https://doi.org/10.1002/1521-3935(20001001)201:15<2008::AID-MACP2008>3.0.CO;2-H).

Sen, Sanghamitra, James D. Martin, and Dimitris S. Argyropoulos. 2013. “Review of Cellulose Non-Derivatizing Solvent Interactions with Emphasis on Activity in Inorganic Molten Salt Hydrates.” *ACS Sustainable Chemistry & Engineering* 1 (8). American Chemical Society: 858–70. <https://doi.org/10.1021/sc400085a>.

Sixta, Herbert, Anne Michud, Lauri Hauru, Shirin Asaadi, Yibo Ma, Alistair W T King, Ilkka Kilpeläinen, and Michael Hummel. 2015a. “Special Issue: CELLULOSE DISSOLUTION AND REGENERATION: SYSTEMS AND INTERACTIONS Ioncell-F: A High-Strength Regenerated Cellulose Fibre.” *Nordic Pulp & Paper Research Journal* 30 (1).

https://www.researchgate.net/profile/Shirin_Asaadi/publication/281961951_Ioncell-F_A_High-strength_regenerated_cellulose_fibre/links/562f3fd508ae22b17036d081/Ioncell-F-A-High-strength-regenerated-cellulose-fibre.pdf.

———. 2015b. “Special Issue: CELLULOSE DISSOLUTION AND REGENERATION: SYSTEMS AND INTERACTIONS Ioncell-F: A High-Strength Regenerated Cellulose Fibre.” *Nordic Pulp & Paper Research Journal* 30 (1).

https://www.researchgate.net/profile/Shirin_Asaadi/publication/281961951_Ioncell-F_A_High-strength_regenerated_cellulose_fibre/links/562f3fd508ae22b17036d081/Ioncell-F-A-

High-strength-regenerated-cellulose-fibre.pdf.

- . 2015c. “Special Issue: CELLULOSE DISSOLUTION AND REGENERATION: SYSTEMS AND INTERACTIONS Ioncell-F: A High-Strength Regenerated Cellulose Fibre.” *Nordic Pulp & Paper Research Journal* 30 (1).
https://www.researchgate.net/profile/Shirin_Asaadi/publication/281961951_Ioncell-F_A_High-strength_regenerated_cellulose_fibre/links/562f3fd508ae22b17036d081/Ioncell-F-A-High-strength-regenerated-cellulose-fibre.pdf.
- Struszczyk, H, D Ciechańska, D Wawro, P Nousiainen, and M Matero. 1995. “Direct Soluble Cellulose of Celsol: Properties and Behaviour.” In *Cellulose and Cellulose Derivatives*, 29–35. Elsevier. <https://doi.org/10.1533/9781845698539.1.29>.
- Wanasekara, Nandula D., Anne Michud, Chenchen Zhu, Sameer Rahatekar, Herbert Sixta, and Stephen J. Eichhorn. 2016a. “Deformation Mechanisms in Ionic Liquid Spun Cellulose Fibers.” *Polymer* 99 (September). Elsevier: 222–30.
<https://doi.org/10.1016/J.POLYMER.2016.07.007>.
- . 2016b. “Deformation Mechanisms in Ionic Liquid Spun Cellulose Fibers.” *Polymer* 99 (September). Elsevier: 222–30.
<https://doi.org/10.1016/J.POLYMER.2016.07.007>.
- Wang, Hui, Gabriela Gurau, and Robin D. Rogers. 2012. “Ionic Liquid Processing of Cellulose.” *Chemical Society Reviews* 41 (4). The Royal Society of Chemistry: 1519.
<https://doi.org/10.1039/c2cs15311d>.
- Wang, Jinwu, Douglas J. Gardner, Nicole M. Stark, Douglas W. Bousfield, Mehdi Tajvidi, and Zhiyong Cai. 2018. “Moisture and Oxygen Barrier Properties of Cellulose Nanomaterial-Based Films.” *ACS Sustainable Chemistry & Engineering* 6 (1): 49–70.
<https://doi.org/10.1021/acssuschemeng.7b03523>.
- Wang, S, A Lu, L Zhang - Progress in Polymer Science, and undefined 2016. n.d. “Recent Advances in Regenerated Cellulose Materials.” *Elsevier*. Accessed April 26, 2018.
<https://www.sciencedirect.com/science/article/pii/S007967001500074X>.

Wawro, D, M Hummel, ... A Michud - *Fibres & Textiles in, and undefined* 2014. n.d.

“Strong Cellulosic Film Cast from Ionic Liquid Solutions.” *Yadda.Icm.Edu.Pl.*

Accessed May 8, 2018.

<http://yadda.icm.edu.pl/baztech/session.action?userAction=property¶meterName=search%2FitemsPerPage¶meterValue=50¤tUrl=%2Fbaztech%2Felement%2Fbwmeta1.element.baztech-16e6bd22-8ae0-46d9-a093-d5217d14d481¤tApplicationPath=%2Felement%2Fbwmeta1.element.baztech-16e6bd22-8ae0-46d9-a093-d5217d14d481&selectResultsNumber=50>

Wawro, D, W Stęplewski, ... W Madaj - *Fibres & Textiles in, and undefined* 2015. n.d.

“Impact of Water in the Casting of Cellulosic Film from Ionic Liquid Solutions.”

Yadda.Icm.Edu.Pl. Accessed May 9, 2018.

<http://yadda.icm.edu.pl/baztech/session.action?userAction=property¶meterName=search%2FitemsPerPage¶meterValue=100¤tUrl=%2Fbaztech%2Felement%2Fbwmeta1.element.baztech-912c29fd-c93d-4b60-a82f-89d15f640266¤tApplicationPath=%2Felement%2Fbwmeta1.element.baztech-912c29fd-c93d-4b60-a82f-89d15f640266&selectResultsNumber=100>

Woodings, Calvin., and England) Textile Institute (Manchester. 2001. *Regenerated Cellulose Fibres*. CRC Press. https://books.google.fi/books?op=lookup&id=U-akAgAAQBAJ&continue=https://books.google.fi/books%3Fhl%3Den%26lr%3D%26id%3DU-akAgAAQBAJ%26oi%3Dfnd%26pg%3DPA37%26dq%3Dviscose%2Bprocess%26ots%3DGr2MFr2Xoe%26sig%3Dz789niGsvHx9T8mMDo7NKABjmeQ%26redir_esc%3Dy

Xu, Airong, Lin Chen, and Jianji Wang. 2018. “Functionalized Imidazolium Carboxylates for Enhancing Practical Applicability in Cellulose Processing.” *Macromolecules* 51 (11). American Chemical Society: 4158–66.

<https://doi.org/10.1021/acs.macromol.8b00724>.

Xu, Y., Z. Lu, and R. Tang. 2007. “Structure and Thermal Properties of Bamboo Viscose, Tencel and Conventional Viscose Fiber.” *Journal of Thermal Analysis and*

Calorimetry 89 (1): 197–201. <https://doi.org/10.1007/s10973-005-7539-1>.

Yang, Quanling, Shuji Fujisawa, Tsuguyuki Saito, and Akira Isogai. 2012. “Improvement of Mechanical and Oxygen Barrier Properties of Cellulose Films by Controlling Drying Conditions of Regenerated Cellulose Hydrogels.” *Cellulose* 19 (3). Springer Netherlands: 695–703. <https://doi.org/10.1007/s10570-012-9683-7>.

Yang, Quanling, Hayaka Fukuzumi, Tsuguyuki Saito, Akira Isogai, and Lina Zhang. 2011a. “Transparent Cellulose Films with High Gas Barrier Properties Fabricated from Aqueous Alkali/Urea Solutions.” *Biomacromolecules* 12 (7). American Chemical Society: 2766–71. <https://doi.org/10.1021/bm200766v>.

———. 2011b. “Transparent Cellulose Films with High Gas Barrier Properties Fabricated from Aqueous Alkali/Urea Solutions.” *Biomacromolecules* 12 (7): 2766–71. <https://doi.org/10.1021/bm200766v>.

Zhang, Jinming, Hao Zhang, Jin Wu, Jun Zhang, Jiasong He, and Junfeng Xiang. 2010. “NMR Spectroscopic Studies of Cellobiose Solvation in EmimAc Aimed to Understand the Dissolution Mechanism of Cellulose in Ionic Liquids.” *Physical Chemistry Chemical Physics* 12 (8). The Royal Society of Chemistry: 1941. <https://doi.org/10.1039/b920446f>.

Zhang, Shaokai, Chunxia Chen, Chao Duan, Huichao Hu, Hailong Li, Jianguo Li, Yishan Liu, Xiaojuan Ma, Jaroslav Stavik, and Yonghao Ni. 2018a. “Regenerated Cellulose by the Lyocell Process, a Brief Review of the Process and Properties.” *BioResources* 13 (2). <https://doi.org/10.15376/biores.13.2>.

———. 2018b. “Regenerated Cellulose by the Lyocell Process, a Brief Review of the Process and Properties.” *BioResources* 13 (2). <https://doi.org/10.15376/biores.13.2>.

Zhu, S, Y Wu, Q Chen, Z Yu, C Wang, S Jin, ... Y Ding - Green, and undefined 2006. n.d. “Dissolution of Cellulose with Ionic Liquids and Its Application: A Mini-Review.” *Pubs.Rsc.Org*. Accessed April 24, 2018. <http://pubs.rsc.org/en/content/articlehtml/2006/gc/b601395c>.

Zhu, Shengdong, Yuanxin Wu, Qiming Chen, Ziniu Yu, Cunwen Wang, Shiwei Jin,

Yigang Ding, and Gang Wu. 2006. "Dissolution of Cellulose with Ionic Liquids and Its Application: A Mini-Review." *Green Chemistry* 8 (4). The Royal Society of Chemistry: 325. <https://doi.org/10.1039/b601395c>.

Appendix 1. Mechanical properties of regenerated films from recent publications.

Solvent system	Process method	Tensile strength (MPa)	Elongation (%)	Young's Modulus (GPa)	Reference
NMMO	Blown	50-300	2-24	1-3	(H. P. Fink et al. 2001)
NaOH/urea	Cast	75-138	4-8		(Qi, Chang, and Zhang 2009)
NaOH/urea	Cast	80-110	15-20		(Lina Zhang et al. 2005)
NaOH/thiourea	Cast	1.97	192		(Liang et al. 2007)
[emim]OAc	Cast	105	7.6		(Pang et al. 2015)
NaOH/urea	Cast	85-139	2-3		(Li et al. n.d.)
[emim]OAc	Cast	87-105	10-50	2-10	(Wawro, Stęplewski, et al. n.d.)

Appendix 2. Regenerated cellulose films produced by spinning in detail

Component	Mass/g	Dry matter content/%	Concentration/%
Enocell	140.85	92.16	7.95
[DBNH][OAc]	1492.92		92.05

Parameter						
Spinneret Diameter/mm	0.1*60*1.0					
Spinning temperature/°C	55					
Extrusion velocity/m*min ⁻¹	2.1167					
Spinneret pressure/Pa	58.8	58	59	59.2	58	58.4
Godet velocity/ m*min ⁻¹	2.2	2.5	3.5	4	5	7.5
Draw ratio	1.04	1.18	1.65	1.89	2.36	3.54

